WATER RESOURCES RESEARCH, VOL. 33, NO. 1, PAGES 91–109, JANUARY 1997

Hydrologic response of a steep, unchanneled valley to natural and applied rainfall

David R. Montgomery,[1] William E. Dietrich,[2] Raymond Torres,[2] Suzanne Prestrud Anderson,[2,3] John T. Heffner,[4] and Keith Loague[5]

Abstract. Observations from natural rain storms and sprinkling experiments at a steep zero-order catchment in the Oregon Coast Range demonstrate the importance of flow through near-surface bedrock on runoff generation and pore pressure development in shallow colluvial soils. Sprinkling experiments, involving irrigation of the entire 860 m^2 catchment at average intensities of 1.5 and 3.0 mm/h, permitted detailed observation of runoff and the development of subsurface saturation under controlled conditions. A weir installed to collect flow through the colluvium at the base of the catchment recovered runoff equal to one third to one half of the precipitation rate during quasi-steady irrigation. Three key observations demonstrate that a significant proportion of storm runoff flows through near-surface bedrock and illustrate the importance of shallow bedrock flow in pore pressure development in the overlying colluvial soil: (1) greater discharge recovery during both the experiments and natural rainfall at a weir installed approximately 15 m downslope of the weir at the base of the catchment, (2) spatially discontinuous patterns of positive pressure head in the colluvium during steady sprinkling, and (3) local development of upward head gradients associated with flow from weathered rock into the overlying colluvium during high-intensity rainfall. Data from natural storms also show that smaller storms produce no significant runoff or piezometric response and point to a critical intensity-duration rainfall to overcome vadose zone storage. Together these observations highlight the role of interaction between flow in colluvium and near-surface bedrock in governing patterns of soil saturation, runoff production, and positive pore pressures.

Introduction

The translation of rainfall into runoff occurs by a variety of mechanisms associated with different environments. Horton overland flow (HOF) occurs primarily in arid or disturbed landscapes where rainfall intensity exceeds the infiltration rate of the surface soil long enough for ponding to occur [*Horton*, 1933]. Recognition of the rarity of HOF in humid, soil-mantled landscapes led to the proposal of subsurface flow as a major mechanism of storm runoff [*Loudermilk*, 1934; *Hursh*, 1936; *Whipkey*, 1965; *Hewlett and Hibbert*, 1967]. Subsurface storm flow (SSSF) dominates runoff generation in steep soil-mantled terrain where precipitation infiltrates and flows laterally either through macropores or over a lower conductivity zone, such as at the base of a root mat or at the soil/bedrock boundary. Saturation overland flow (SOF) occurs in soil-mantled landscapes when an initially shallow water table intersects the ground surface over a portion of the catchment [*Hewlett and Hibbert*, 1967], causing runoff by either return flow or direct precipitation onto saturated areas [*Dunne and Black*, 1970]. Topographically driven patterns of soil moisture favor development of SOF in low-gradient, convergent topography [e.g., *Beven and Kirkby*, 1979]. Groundwater flow (GWF) contributes to discharge recession and maintains base flow, but many workers consider flow through bedrock a negligible influence on storm flow [e.g., *Likens et al*., 1977; *Mulholland*, 1993]. *Wilson et al*. [1990] demonstrated through field observations and numerical simulations that the magnitude of the conductivity contrast dictated the coupling of flow between colluvial soil and the underlying bedrock. Hence the relative importance of these runoff generation mechanisms depends on several key ratios: high rainfall intensity to infiltration rate favors HOF, high contributing area to local slope favors SOF, high bedrock to soil permeability favors GWF, and low values of all three ratios favor SSSF.

Runoff generation in steep, soil-mantled landscapes in humid-temperate environments occurs primarily by subsurface flow because rainfall intensities only rarely exceed infiltration capacities [*Dunne*, 1978]. Monitoring studies of runoff generation on steep slopes have focused on mechanisms for rapid subsurface storm flow [e.g., *Mosley*, 1979; *Sklash et al*., 1986; *McDonnell*, 1990] and the positive pore pressures that control shallow landsliding [e.g., *Swanston*, 1970; *Yee and Harr*, 1977; *Pierson*, 1980; *Tsukamoto et al*., 1982; *Sidle*, 1984; *Tsukamoto and Ohta*, 1988; *Johnson and Sitar*, 1990], which represents a significant hazard to life, property, and natural resources in mountainous terrain. Processes influencing shallow landsliding

[1]Department of Geological Sciences, University of Washington, Seattle.
[2]Department of Geology and Geophysics, University of California, Berkeley.
[3]Now at Department of Earth Sciences, University of California, Santa Cruz.
[4]Environmental Research, Weyerhaeuser Company, Centralia, Washington.
[5]Department of Geological and Environmental Sciences, Stanford University, Stanford, California.

Paper number 96WR02985.
0043-1397/97/96WR-02985$09.00

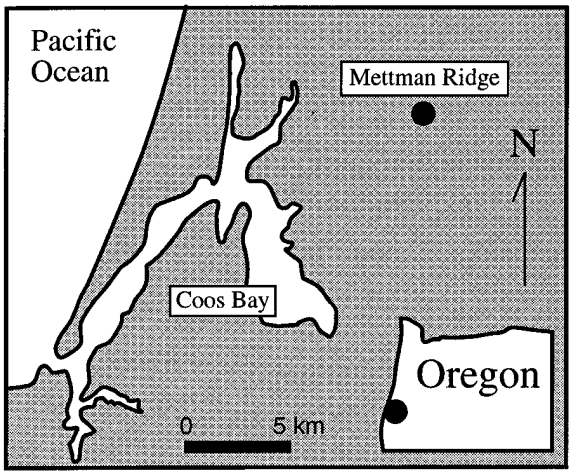

Figure 1. Location map for the Mettman Ridge study site.

impose important controls on landscape evolution in steep, soil-mantled terrain [e.g., *Dietrich and Dunne*, 1978; *Okunishi and Iida*, 1981; *Tsukamoto et al*., 1982; *Dietrich et al*., 1986; *Onda*, 1994], while slope form, in turn, strongly influences near-surface hydrologic response [e.g., *Dunne et al*., 1975; *Anderson and Burt*, 1978; *Bonell and Gilmour*, 1978; *Pierson*, 1980; *Tanaka*, 1982; *Burt and Butcher*, 1986]. This feedback between slope form, runoff generation, and shallow landsliding is fundamental to understanding the geomorphology of mountain drainage basins.

Assumptions about mechanisms of pore pressure generation underlie a wide range of theoretical and applied models for runoff production, slope stability, and landscape evolution. Perched water tables and positive pore pressures result from infiltration to an impeding layer, generally assumed to be either less conductive soil or impermeable bedrock. Such simplifications drive topographically driven models for runoff generation [e.g., *Beven and Kirkby*, 1979; *O'Loughlin*, 1986] that have been extended to predict locations prone to shallow landsliding [e.g., *Dietrich et al*., 1992; *Montgomery and Dietrich*, 1994; *Wu and Sidle*, 1995]. Field observations of fresh debris flow scarps, however, suggest that flow through bedrock fractures can control shallow landslide initiation [e.g., *Pierson*, 1977; *Everett*, 1979; *Mathewson et al*., 1990]. Hydrological field studies also suggest an influence of bedrock properties on pore pressure generation and storm runoff [*Pierson*, 1980; *Hammermeister et al*., 1982; *Wilson and Dietrich*, 1987; *Terajima and Moroto*, 1990; *Wilson et al*., 1993]. Here we report evidence for a significant influence of shallow bedrock flow on runoff and piezometric response to natural rainfall and two whole-catchment sprinkling experiments during an integrated study of runoff generation, slope stability, and landscape evolution at an intensively instrumented catchment in the Oregon Coast Range.

Study Area and Experimental Design

We selected the Oregon Coast Range for our study because of extensive prior work in this area and the feasibility of conducting whole-catchment sprinkling experiments in small, steep unchanneled valleys. Convergence of subsurface flow makes steep channel heads especially prone to instability and contributes to the cycle of periodic colluvial infilling and excavation by shallow landsliding in the hollows that feed the channel network [*Dietrich and Dunne*, 1978; *Dietrich et al*., 1986]. Debris flows originating in hollows can scour low-order channels and deliver substantial sediment pulses to downstream channels; shallow landsliding dominates sediment transport in the steep headwater valleys [e.g., *Dietrich and Dunne*, 1978; *Benda*, 1990]. Recent timber harvesting and road construction dramatically accelerated rates of slope failure in the Oregon Coast Range [*Fredriksen*, 1970; *Brown and Krygier*, 1971; *Mersereau and Dyrness*, 1972; *Swanston and Swanson*, 1976; *Gresswell et al*., 1979].

The Mettman Ridge study area is located approximately 15 km northeast of Coos Bay, Oregon (Figure 1), at an elevation of approximately 300 m on the crest of the first major ridgeline inland from the Pacific Ocean. Mettman Ridge was selected because it offered ridgetop road access to small, steep catchments, had ridge crest logging landings ideal for staging sprinkling experiments, and was near a quarry pond available as a source of sprinkler water. Two neighboring catchments (CB1 and CB2) were selected for the study (Plate 1 and Figure 2). The CB1 catchment consists of the drainage area contributing to a channel head, while the CB2 catchment also contains a 15-m-long section of a first-order bedrock channel. Postharvest rates of shallow landsliding along Mettman Ridge greatly ex-

Plate 1. Mettman Ridge study area. White RV is parked at head of CB1. Yellow object and brown cylinder on ridge crest landing at right are water tanks used during sprinkling experiments. Note debris-flow scar resulting from ridgetop road drainage into hollow to the left of CB1.

ceed long-term rates [*Montgomery*, 1991], and many of the slides in this area result from concentration of drainage along the ridgetop road system [*Montgomery*, 1994].

The study sites are typical of steep zero-order catchments in the Oregon Coast Range. Prior to 1987 the area supported a mixed conifer and hardwood forest. Both study sites and their immediate vicinity were clear cut logged in 1987 and replanted with Douglas fir (*Pseudotsuga menziesii*) in 1989. Bedrock in the area consists of relatively undeformed Eocene sandstone [*Dott*, 1966; *Baldwin*, 1974]. Exposures in adjacent debris-flow scars, downslope channels, and road cuts along the ridge crest reveal massive sandstone with minor silty and pebbly interbeds dipping 8°–17° into the slope. The near-surface sandstone appears variably fractured and weathered, although exposures in channelways lower on the slope reveal massive, relatively impermeable bedrock. Soils at the study sites are low-density silty sands mapped as Haplumbrepts in the Bohanon series [*Haagen*, 1989]. Samples collected from a soil pit excavated in CB2 consist of approximately 50% (by weight) fine to coarse sand and 25% each of fine gravel and silt. As is typical in the Oregon Coast Range, thin soil profiles on interfluves yield to thicker soils along hollows. The observation of fresh massive sandstone exposed in nearby debris-flow scars and stream channels led us to expect little bedrock flow at our site, so we concentrated our initial experimental design on documenting the hydrologic response of the loose, highly conductive soil mantle.

Weirs

Three weirs were installed at CB1 and CB2 between 1989 and 1991. Each weir consisted of a v notch flume that was leveled and braced during installation and periodically adjusted to correct for minor settling. Sheet metal molded and nailed to the bedrock surface and quick-set concrete were used to seal each weir to the bedrock surface. All three weirs were equipped with stilling wells, stage recorders accurate to ± 1 mm, and battery-operated data loggers. Coupled discharge and stage measurements obtained during natural rainfall and sprinkler experiments allowed us to generate rating curves for each weir.

The upper weir was installed in 1989 at the channel head at the base of CB1. Installation of the upper weir involved excavating the channel head to bedrock and constructing oblique, upslope-extending weir wings to capture flow through the colluvial soil from the catchment upslope of the channel head. Power drill cuttings from the massive rock encountered at the base of excavations were dry even when water was flowing over the exposed bedrock surface. Localized bedrock fracturing was noted during the installation of the right (facing downslope) weir wing. An automated float-type water-level indicator installed in a stilling well and connected to a data logger has recorded the stage of discharge passing through the weir since January 1990.

The lower weir was automated in October 1991 and is located along the channel approximately 15 m downslope of the upper weir, at the site of a temporary weir improvised in May 1990. The lower weir was constructed by excavating the approximately 0.3-m-thick colluvial valley fill down to bedrock; wing walls were constructed by excavating across the valley bottom and up the valley sides. A polyvinyl chloride (PVC) culvert installed in the channelway routed discharge from both the upper weir and the hollow west of CB1 past the lower weir, which consequently records flow that moves under the upper weir and enters the channel above the lower weir.

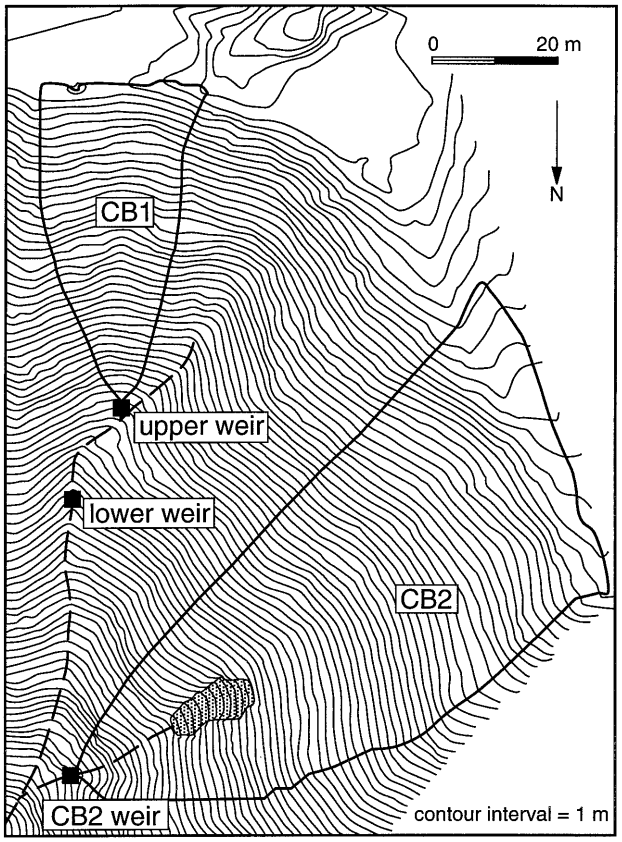

Figure 2. Map showing catchment areas for CB1 and CB2 and the location of the upper, lower, and CB2 weirs (solid boxes). Dashed lines indicate ephemeral channels. Landslide at the channel head of CB2 (shaded area) occurred in February 1992.

The CB2 weir was installed in 1989 along the 40°–43° bedrock channel approximately 15 m downslope of the channel head; no other instrumentation was installed in CB2. The CB2 weir was anchored by bolting a frame to the rock surface and cantilevering the flume out from the slope. The upper and lower weirs are still (1996) recording and the CB2 weir recorded until it was destroyed by a debris flow originating at the upslope channel head in February 1992.

CB1 Catchment

The CB1 catchment consists of an 860 m^2 source area on a 43° slope. Installation of significant infrastructure at CB1 allowed repeated access to instrumentation without excessive ground disturbance (Figure 3). Stairs and trails constructed down the eastern topographic nose access a network of suspended platforms that are anchored where possible onto fallen logs or laid directly on the slope where no support was available.

An extensive array of instrumentation was installed in CB1 under the expectation of rapid flow through soil above less conductive bedrock. We installed 195 piezometers in hand-auger borings distributed in 86 nests across the site. Piezometers consist of a 25.4-mm-diameter PVC pipe, with hacksaw slots cut in the lowest 0.10 m. PVC caps installed at the base of the piezometers to prevent clogging preclude observation of saturated zones less than about 0.03 m thick. Bentonite was used to seal borings above sand emplaced around the slotted

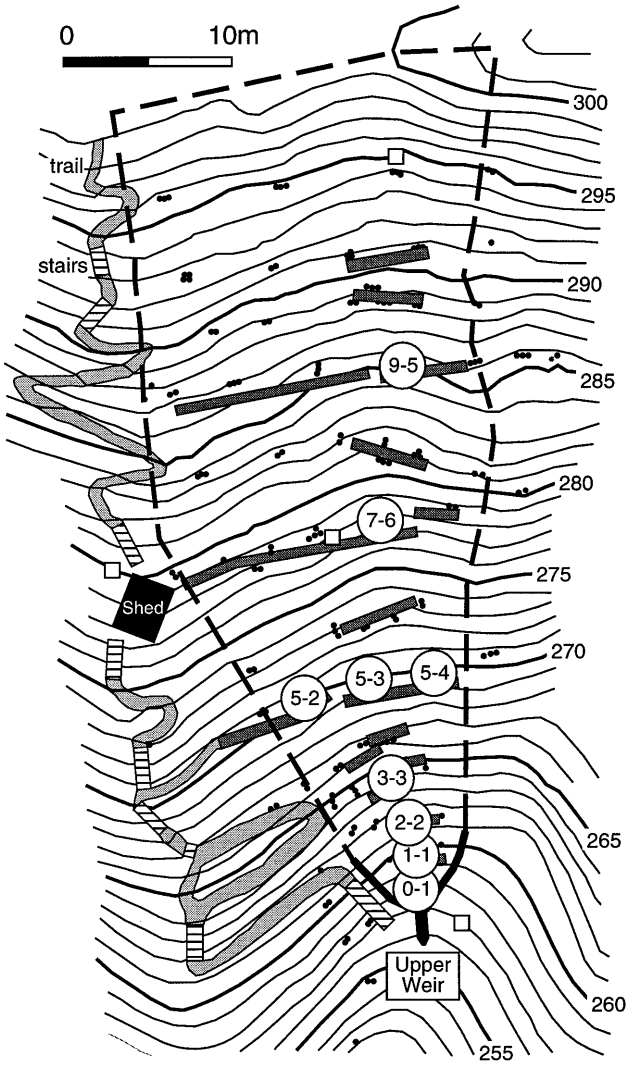

Figure 3. Map showing site infrastructure and location of automated (labeled circles) and manual (small solid dots) piezometers and automated rain gauges (open squares). Shaded rectangles represent platforms. North is to the bottom of the figure.

interval; boring backfill consisted of native materials capped with bentonite at the ground surface. Within a nest, piezometers were installed at approximately half-meter depth intervals, with the deepest piezometer at the local limit of hand auger penetration. Twenty-three piezometers were installed into weathered rock, the remainder being installed in colluvium.

Twenty-two piezometers in nine nests were instrumented with pressure transducers; two were installed in weathered rock, the rest being installed in colluvium. Data loggers recorded pressure head in automated nests over 10-min intervals during both sprinkling experiments and natural storms. During sprinkling experiments, manual piezometric measurements collected several times a day with an electronic water level meter accurate to ± 0.01 m supplemented the automated data.

Soil-auger samples described during piezometer installation revealed little textural variation within the colluvial soil, although soil thickness varied substantially. In general, an organic-rich A horizon overlies a brown gravelly silty sand, and a variable thickness of augerable weathered rock locally underlies the colluvial soil. Generalized isopachs of colluvium thickness encountered during installation of each piezometer nest mask some local variability but show that soil depth varies from <0.5 m on the noses to almost 2.0 m locally along the hollow axis (Figure 4). Colluvium thickness averages about 1.4 m along the hollow axis, thinning rapidly downslope at the base of the hollow. Weathered bedrock was recovered in some hand-auger borings, but in many nests the deepest borings were interpreted as terminating at competent rock below the colluvial deposit. Some borings stopped when sandstone encountered in the first half meter prevented further drilling, even though adjacent borings indicated colluvium depths greater than 1 m. We interpret this variability to primarily reflect that sandstone fragments are distributed throughout the soil profile, although there is irregularity to the colluvium/bedrock contact.

In the fall of 1990 and the spring of 1991, 28 borings ranging from 0.35 to 5.05 m in depth were drilled into bedrock using a hand-held posthole digger modified for diamond-bit coring [*MacDonald*, 1988]. A 35-m-deep well was drilled on the ridge crest shoulder at the head of CB1 using a truck-mounted diamond-bit coring rig. Core recovery from bedrock borings indicated that the thick weathered and fractured bedrock at the ridge crest thins downslope (Figure 5).

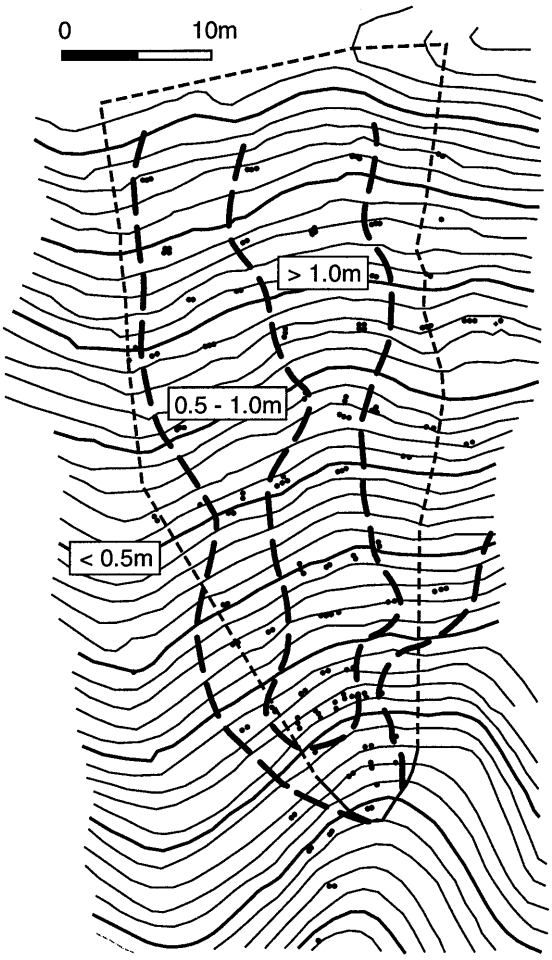

Figure 4. Generalized map of soil depth inferred from hand-auger borings at each piezometer nest.

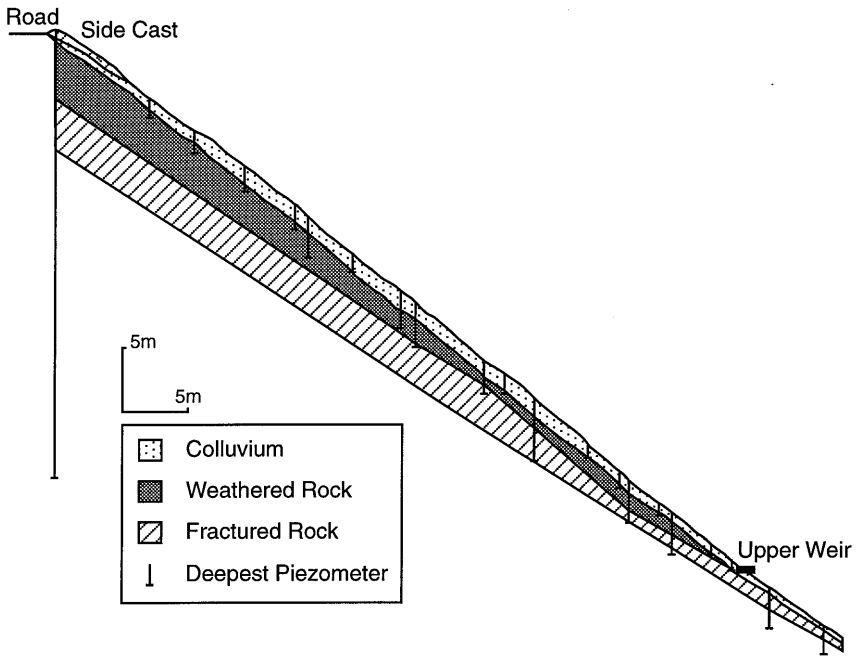

Figure 5. Long profile down the axis of the topographic hollow showing stratigraphy interpreted from bedrock drilling.

These bedrock piezometer installations were done after the experiments and monitoring discussed here but allow a detailed description of the bedrock. As core recovery was greater than 90% over the interval from 3 to 35 m in the ridge crest boring, our interpretation is based heavily on that core and was extended downslope with the more fragmentary recovery in the power-auger holes shown in Figure 5. The weathered rock layer is light brown to tan in color and variably fractured. At locations near the ridge crest it is possible to hand auger up to 1.5 m into this layer, while near the channel head, a hand auger cannot penetrate it. Fractures with oxidation staining are common and increase in number toward the surface. These probably represent hydrologically active exfoliation fractures. Below this, both gray unweathered rock and tan to brown oxidized rock occur together in the fractured rock layer, which is at most 4.5 m thick. Open, high-angle fractures, surrounded by oxidation halos tens of millimeters thick, cut through the competent unweathered rock. Examples of this juxtaposition of unweathered and oxidized rock were found close to the surface in cores at the base of the slope, suggesting the thinning of the layers shown in Figure 5. Below this fractured zone the rock is essentially unweathered; fractures are fewer in number, and although some have oxidation staining (and even this disappears with depth), none are surrounded by the bands of oxidized rock seen in the overlying fractured rock.

Other instrumentation included a network of recording and manual rain gauges and a tensiometer array. Data loggers recorded rainfall over 10-min intervals collected in tipping bucket rain gauges located at the top, middle, and bottom of the site. Sprinkler experiments included an additional automated rain gauge near piezometer nest 7-6. During the sprinkler experiments, irrigation was measured in 137 wedge-type rain gauges distributed across the site on short stakes driven into the ground. For the sprinkling experiments, total site irrigation was estimated for approximately 12-hour periods as the mean of the manual rain gauge readings. A recording weather station installed during the experiments recorded wind velocity and direction, solar radiation, and air temperature.

Falling head conductivity tests [*Hvorslev*, 1951] were conducted in 31 piezometers prior to the sprinkler experiments. Conductivity measurements prior to the sprinkling experiments incorporated 74 tests conducted in 28 piezometers installed in soil and three installed in weathered rock. The tests were conducted by filling a piezometer with water and then monitoring the water level with a pressure transducer and data logger at 5-s intervals to the nearest 0.01 m. Water levels in more slowly draining piezometers were read intermittently using a water-depth probe. Saturated conductivities calculated for piezometers with inlets in colluvium vary systematically from about 10^{-3} m/s near the ground surface to about 10^{-4} m/s at 2-m depth (Figure 6). The four conductivity values from

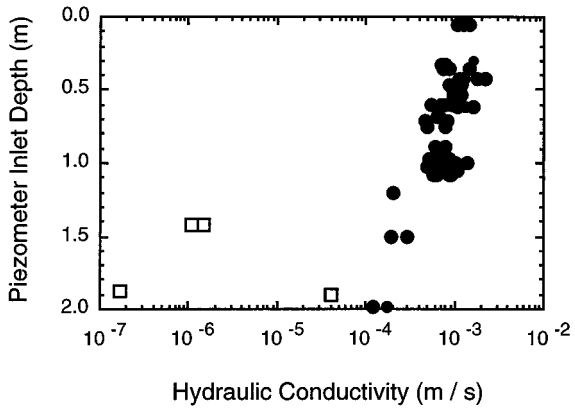

Figure 6. Hydraulic conductivity versus piezometer inlet depth. Solid circles are for piezometers with inlets in colluvium; open squares are for weathered rock.

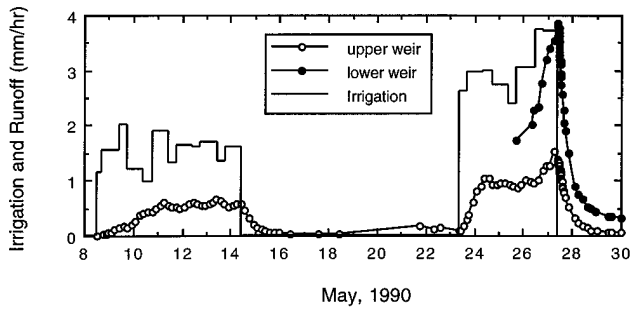

Figure 7. Average irrigation rates and runoff rates from hand-collected discharge data for the upper and lower weirs during sprinkling experiments.

piezometers installed into the weathered bedrock range from 10^{-4} to 10^{-7} m/s. Similar soils elsewhere in the Oregon Coast Range exhibit comparable conductivities [*Harr*, 1977; *Yee and Harr*, 1977; *Hammermeister et al*., 1982].

In contrast to the natural storms in which observations were limited to automated instruments, the sprinkling experiments involve comprehensive measurements and visual observations. During the experiments, piezometric, tensiometric, and discharge measurements were obtained and water samples were collected by shifts operating around the clock. Hand measurements of discharge collected during the experiments were more sensitive and accurate than the higher-frequency automated stage data, especially at low discharges.

Sprinkler Experiments

We installed a network of 13 rainbird-type rotating sprinklers mounted approximately 2 m above the ground surface to simulate rainfall under controlled conditions early in May 1990. A main pipe running down the western nose connected to three smaller pipes running across the site, each of which fed a series of sprinklers. A pressure gauge at the end of each of these lines and a pressure valve at its junction with the feeder pipe regulated flow rates. A portable pump fed the main conduit from a 38,000-L storage tank on the ridge crest, which was supplied using a 15,000-L water truck that transported water from a quarry pond several kilometers away.

Irrigation rates for sprinkling experiments were selected to emulate typical storm events while avoiding high pore pressures, which might trigger slope instability. The average rainfall intensities were 1.5 $\pm$ 0.8 mm/h and 3.0 $\pm$ 0.9 mm/h, and total rainfall was 211 $\pm$ 88 mm and 289 $\pm$ 79 mm during experiments 1 and 2. The two experiments are equivalent to $<$1-year and 1- to 2-year 24-hour events respectively, based on records from the nearby North Bend (23 years) and Alleghany (41 years) rain gauges. On the basis of comparison with the Alleghany rain gauge, experiment 1 was equivalent to a 1- to 2-year recurrence interval 6-day rainfall, whereas the shorter duration, higher-intensity experiment 2 was equivalent to a 10- to 15-year recurrence interval 4-day rainfall. Each experiment lasted long enough to sustain a quasi-steady discharge for several days.

During the experiments, variations in irrigation intensity occurred around sprinkler heads and from changes in wind intensity. During periods of high wind velocity (usually in the afternoon and early evening), some water from the sprinklers was entrained and blown off of the site. Although sprinklers operated at a nearly constant flow, variations in irrigation at the ground surface likely contributed to diurnal variations in pressure head and discharge.

Runoff Response

No overland flow occurred during the low-intensity, long-duration irrigation applied during the sprinkler exeriments. Discharge response to both steady sprinkler experiments exhibited a gradual rise once irrigation began, eventually reached a relatively steady discharge, and decayed once the water was turned off (Figure 7). Discharge at the upper weir increased slowly from the start of sprinkling at noon on May 8. Approximately steady state discharge began around midnight on May 11 and lasted until the sprinklers were shut off at 10 A.M. on May 14. Discharge began decreasing upon termination of irrigation and response to experiment 1 ended by about 11 A.M. May 16. On May 21 and 22, 39 mm of natural rain fell at intensities up to 7.9 mm/h and produced minor runoff response. Experiment 2 began at 9:30 A.M. on May 23 and lasted 4 days. Discharge rose more rapidly than in experiment 1, reaching a near–steady state response after approximately 1 day. Diurnal discharge oscillations about steady state persisted for 2 days until natural rainfall supplemented the irrigation on May 26 and 27. Natural rainfall ended shortly before sprinklers were shut off at 9:30 A.M. on May 27, and again, discharge through the upper weir returned to the preexperiment level within 2 days.

Comparison of the irrigation rate to discharge through the upper weir reveals that runoff through the colluvial soil accounted for only a portion of the irrigation during the sprinkling experiments (Figure 7). During quasi-steady response in experiment 1 the automated discharge record for the upper weir ranged between 0.50 and 0.66 mm/h, corresponding to 33–44% of the irrigation rate (1.5 mm/h). During experiment 2 the steady state discharge ranged beween 0.86 and 1.04 mm/h, corresponding to 29–35% of the irrigation rate (3.0 mm/h). Runoff coefficients (ratio of total runoff to irrigation) for the upper weir were 0.32 and 0.36 for experiments 1 and 2, respectively. The temporary lower weir installed on May 25 captured runoff from the upper weir, the neighboring hollow at the head of the channel (which was not irrigated), and runoff that flowed under the upper weir to emerge along the downslope channel. This temporary weir recovered 1.74–2.34 mm/h, corresponding to 58–78% of the irrigation rate, during the first four measurements obtained during the sprinkling experiments. Later, when sprinkling was augmented by natural rainfall on May 26 and 27, discharge exceeded the irrigation rate due to the contribution of rainfall onto areas neighboring CB1.

Diurnal discharge oscillations, with daily maxima occurring in the midmorning, likely reflect the combined influence of vigorous understory vegetation and variations in the amount of irrigation blown off site by afternoon wind. Discharge oscillations of 0.11–0.12 mm/h at steady state response during the first experiment correspond to 7–8% of the irrigation rate. During the second experiment the discharge recovery at steady state response varied by 0.08–0.14 mm/h, equivalent to 3–5% of the irrigation rate. A tower located approximately in the center of the experimental site measured an average evaporation rate of 0.25 mm/h at CB1 during sprinkler experiments with comparable rainfall intensities in May–June 1992 (T. Giambelluca, personal communication, 1996). Assuming little leakage to deeper groundwater, evapotranspiration likely ac-

counted for 5–20% of the rain falling on the study sites during the sprinkling experiments.

Piezometric Response

Water levels measured in piezometers record pressure head Ψ, but water flows from areas of high to low total head h, equal to the sum of pressure head and elevation head z. Pore water pressure p, which influences slope stability, is related to pressure head by $p = \rho g \Psi$, where ρ is the fluid density and g is gravitational acceleration. Our discussion will shift among these attributes as we focus on observations (pressure head), implied flow directions (total head), and implications for slope stability (pore pressure). We also adopt the definition of recharging piezometric gradients to refer to flow from colluvium into the underlying bedrock and discharging gradients for the converse case.

Piezometric response during the sprinkling experiments fell within the range recorded during natural storms from January through April 1990. Positive pore pressures during the sprinkling experiments occurred along the hollow axis and increased steadily once initiated. Although pressure head varied in magnitude, consistent sequencing and spatial patterns of response developed in the two experiments. Our analysis concentrates on the more detailed record from the automated piezometers and uses observations from the manual piezometers primarily to examine spatial patterns of response.

Experiment 1. During experiment 1, positive pore pressures occurred in 28 piezometers, distributed among 23 nests. The timing and magnitude of piezometric response varied along the hollow axis (Figure 8). Discharging head gradients developed at nest 0-1 during both rising and falling response, but head gradients were approximately hydrostatic (i.e., equal total head in piezometers at different depths) during the intervening period of steady response. In contrast, nest 2-2, located 5 m upslope of the channel head, exhibited recharging gradients throughout the experiment, with a maximum pressure head of 0.04 m in the shallower piezometer. Shorter-duration, 0.01-m amplitude variations indistinguishable from noise in both piezometers at the start of the experiment obscure the timing of initial response at this nest. Nest 3-3, located 8.5 m upslope of the channel head, exhibited a barely resolvable 0.02-m pressure head response; the shallower piezometer in this nest did not respond.

Piezometer nest 5-3, located 14.2 m upslope of the weir, responded with a delayed but abrupt rise in pressure head and exhibited recharging gradients throughout the experiment. Initial response in the piezometer installed at the base of the colluvium occurred 1 hour before initial response in the deeper piezometer installed in weathered rock. Two shallower piezometers in this nest (not shown in Figure 8) did not exhibit positive pressure head during either experiment. Both responsive piezometers exhibited approximately in-phase diurnal pressure head oscillations of 0.02–0.03 m amplitude. The two automated nests located off of the hollow axis (5-2 and 5-4) did not respond to the sprinkling.

Piezometer nest 7-6, located 23.7 m upslope of the weir, exhibited recharging gradients throughout the experiment. Response in this nest initiated in the middle piezometer, installed at the base of the colluvial soil. The first response in the deeper (weathered rock) piezometer lagged by almost 5 hours, and that in the shallowest piezometer occurred 11.2 hours after initial response at the base of the soil. This nest did not exhibit distinct diurnal oscillations apparent in the record from other nests. As in nest 5-3 the two shallowest piezometers in nest 7-6 (not shown in Figure 8) did not respond to either experiment. Automated piezometer nest 9-5, located 33.3 m upslope of the upper weir, also exhibited a rapid rise in pressure head following initial response. At steady discharge, pressure head exhibited two distinct peaks on May 11 and 13. Response in all automated piezometers began decaying shortly after sprinkling terminated.

During experiment 1 the time lag between the start of irrigation and initiation of positive pressure head at automated piezometers along the hollow was highly correlated with soil depth ($R^2 = 0.81$), a relation that records the downward propagation of the rainfall signal through the vadose zone. Initial response of piezometers at depths of about 0.5 m was roughly coincident with the initial rise in discharge from the upper weir, where the soil depth is about 0.6 m. It therefore appears that weir discharge increased upon arrival of the rainfall signal at the base of the soil immediately upslope of the weir. Initial piezometric response progressed downward through the soil at a rate of 1.2×10^{-5} m/s. The systematic upslope thickening of the colluvium along the hollow may lead to a correlation between distance upslope of the upper weir and the time lag between the start of irrigation and initial piezometric response ($R^2 = 0.61$).

The automated piezometer nests document site response along the hollow axis, but the array of piezometers read by hand provides greater spatial coverage. Positive pore pressures were observed in the deepest piezometers in 18 of the manually read piezometer nests; all other piezometers remained dry throughout the experiments. At steady discharge, patches or zones of positive pressure head concentrated along the hollow were separated by areas in which piezometers did not respond (Figure 9a). Distinct zones of saturation were (1) a zone of 0.04- to 0.18-m pressure head response immediately upslope of the channel head, (2) a zone of 0.03- to 0.07-m pressure head downslope of the channel head and outside the sealed weir wings, (3) an apparently small zone of 0.11- to 0.20-m pressure head along the hollow axis at row 5, and (4) a larger area of 0.05- to 0.18-m pressure head along the hollow axis in the upper half of the site. The range of pressure head observed in each of these zones may reflect local variations in both the topography of the soil/bedrock contact and in localized bedrock fracturing. The zone of positive pressure head downslope of the weir wings confirms deeper bedrock storm flow.

Experiment 2. The pattern of piezometric response during experiment 2 was similar to that in experiment 1: pressure head in the automated piezometers rose, reached a quasi-steady state marked by diurnal oscillations, and then fell rapidly at the termination of sprinkling (Figure 10). Superimposed on this pattern was a substantial pressure head increase during natural rainfall on the last day of the experiment. Nest 0-1 responded to the preexperiment rainfall and retained positive pressure heads at the start of the experiment. Discharging piezometric gradients were maintained at this nest throughout experiment 2. The piezometer in nest 1-1 at the base of the colluvial soil, which was not functional during the first experiment, recorded up to 0.10 m of pressure head. This piezometer exhibited weak 0.01- to 0.02-m oscillations at steady response and a slight rise prior to the end of the experiment. As during experiment 1, nest 2-2 exhibited recharging gradients throughout experiment 2, with a maximum pressure head of 0.07 m in the shallower piezometer. Nest 3-3 exhibited up to 0.10 m response during experiment 2.

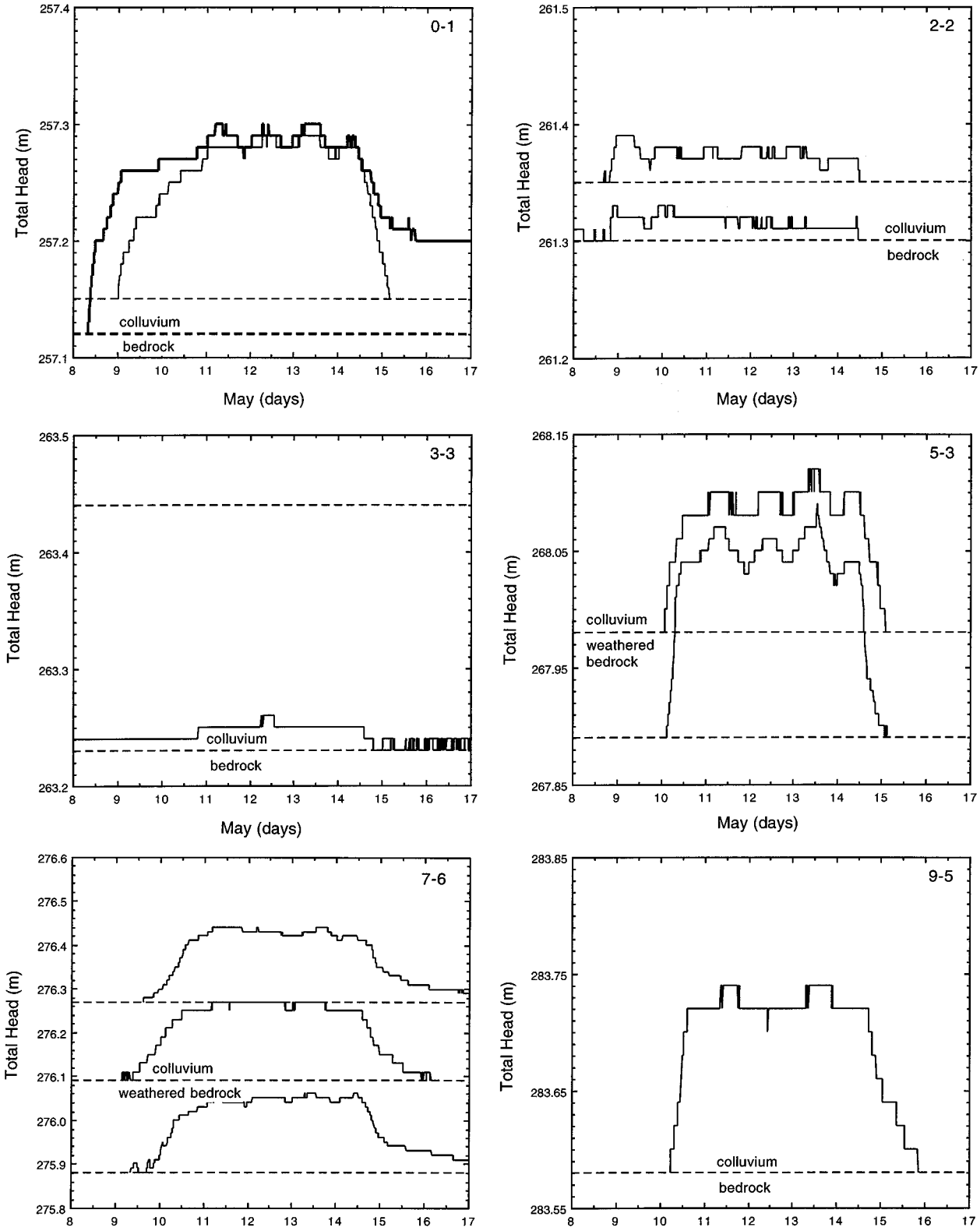

Figure 8. Response of automated piezometers during experiment 1. Numbers in the top right corner of each panel indicate piezometer nest designations. Horizontal dashed lines indicate piezometer inlet elevations (elevation head); pressure head (Ψ) in each piezometer is equal to the difference between total head and the elevation head. Location of the base of the colluvial soil also is indicated.

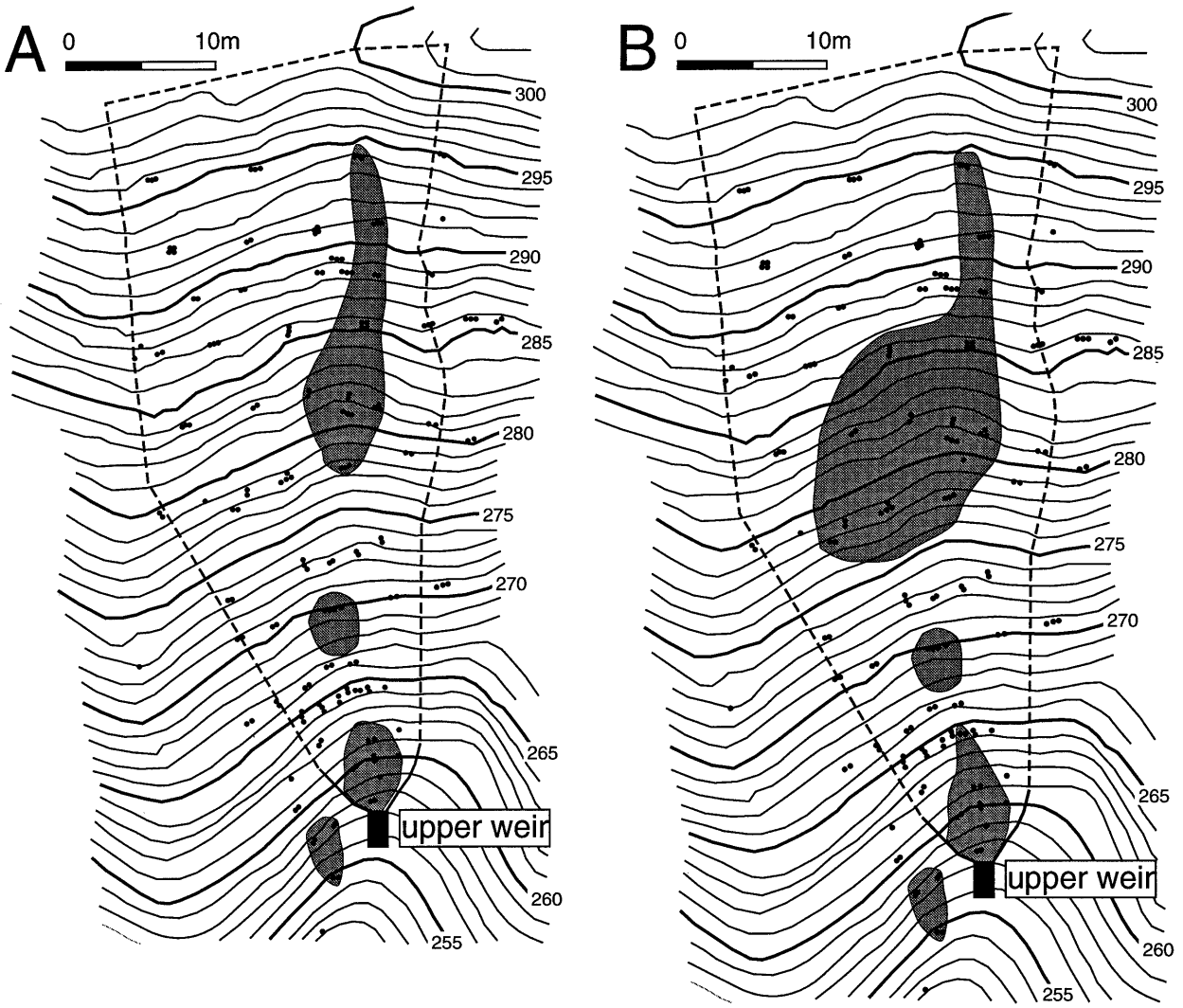

Figure 9. Map of CB1 showing areas of partial soil saturation (shaded areas) during (a) experiment 1 and (b) experiment 2. Dashed line represents contributing area to the upper weir. Small solid dots represent piezometers.

Nest 5-3 responded with a rapid rise in presure head and exhibited recharging gradients throughout experiment 2. Total head gradients, however, approached hydrostatic during the natural rainfall at the end of experiment 2. At this time the deeper weathered rock piezometer rose 0.09 m, whereas the piezometer at the base of the soil rose only 0.02 m. Initial response in the piezometer at the base of the soil and that in the deeper weathered rock piezometer occurred within 10 min of each other. As during experiment 1 the off-axis nests 5-2 and 5-4 did not respond.

At the start of experiment 2, piezometer nest 7-6 retained positive pressure head from the preceding natural rainfall. Initial response of the middle piezometer (installed to the base of the soil) preceded by 1 hour the initial response in both the shallower and deeper piezometers. Again, nest 7-6 did not exhibit distinct pressure head oscillations. Instead, it exhibited relatively steady increases throughout experiment 2. Piezometer nest 9-5, the farthest upslope automated nest, also exhibited a rapid increase in pressure head upon irrigation. In all of the piezometers, response began decaying after the peak rainfall, which occurred approximately 3 hours before irrigation ceased on May 27.

On the basis of nests with multiple responsive piezometers, it appears that piezometric response initiated at the soil/bedrock contact. Data from experiment 2 document a weak correlation between piezometer inlet depth and the time lag from the start of irrigation to initial piezometric response ($R^2 = 0.41$). As gauged by the regressed trend in the time to first response versus piezometer inlet depth, positive pressure head response during experiment 2 progressed down through the colluvium at 1.2×10^{-4} m/s, a rate faster than in experiment 1 and similar to the saturated hydraulic conductivity of the colluvium. In contrast to experiment 1 the time lag to first piezometric response during experiment 2 was independent of position along the hollow ($R^2 = 0.01$).

As in experiment 1, most of the manual piezometers did not exhibit measurable response. The zone of positive pressure head expanded slightly during experiment 2 but consisted of essentially the same zones observed during experiment 1 (Figure 9b). A zone of 0.03- to 0.26-m pressure head developed

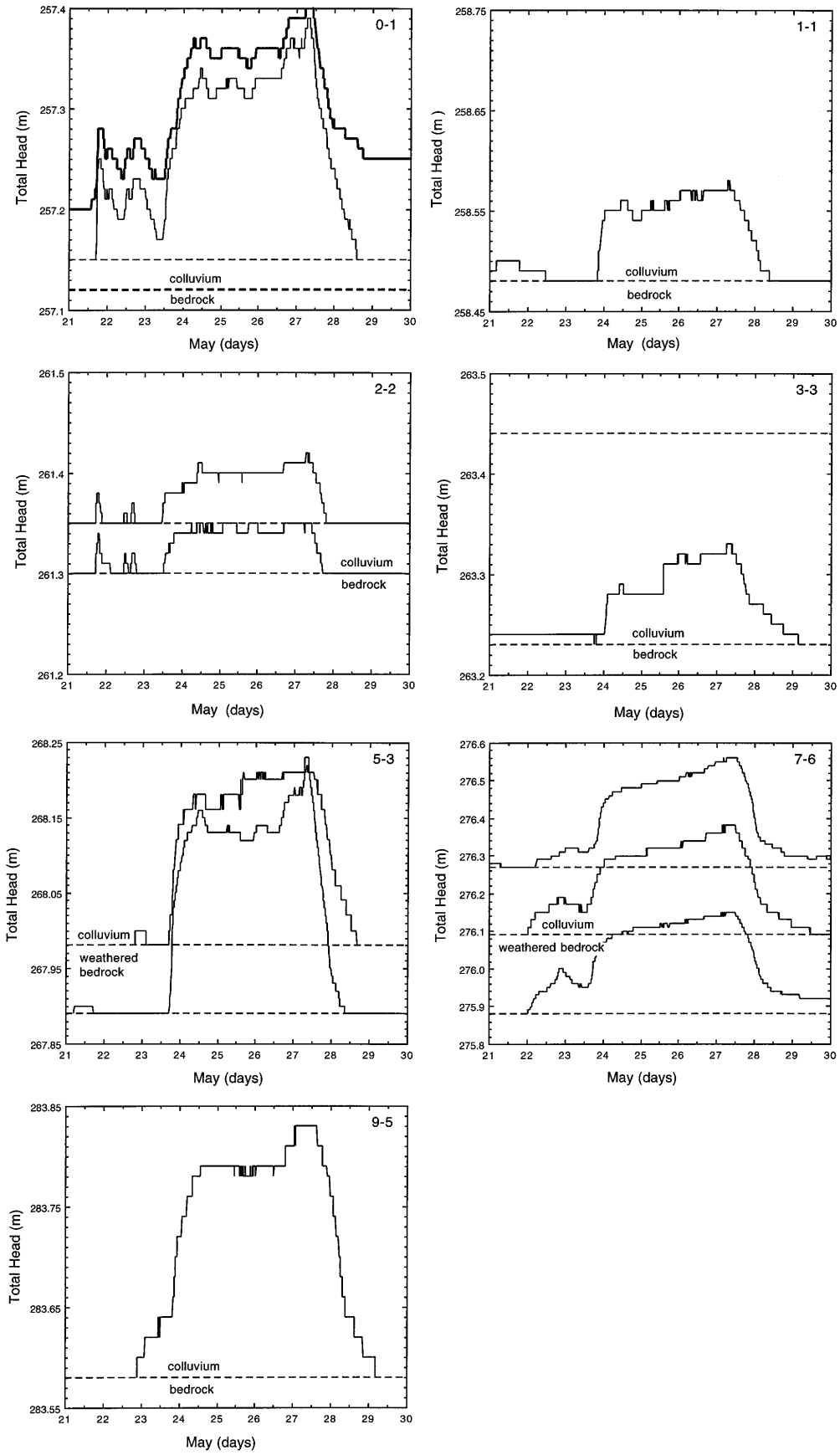

Figure 10. Response of automated piezometers during experiment 2. Horizontal dashed lines indicate piezometer inlet elevations (elevation head); pressure head (Ψ) in each piezometer is equal to the difference between total head and the elevation head.

immediately upslope of the upper weir separated from a small zone of 0.17- to 0.33-m response at and immediately downslope of nest 5-3. Positive pressure head of 0.07–0.15 m developed downslope of the sealed weir wings but laterally offset from the upper weir. The zone of saturated reponse in the upper half of CB1 included both a zone of 0.04- to 0.25-m pressure head in the area along the hollow that responded during experiment 1 and an expanded area of 0.01- to 0.06-m pressure head on the side slopes outside of the topographic hollow. The two zones without saturated response persisted along the hollow.

Natural Rainfall

Overland flow was not observed during site visits during storms in January, February, and April 1990, January 1991, and February 1992. Also, no evidence of overland flow has been observed upslope of the channel head at either site during numerous site visits between storms. The record from automated piezometers shows that saturation never reached the ground surface in CB1 between December 1989 and May 1992; no SOF escaped our observation. Also, the maximum hourly rainfall intensity of 15.5 mm/h during this period lies well below the measured conductivity of near-surface soil of about 3600 mm/h, indicating that no HOF occurred. We repeatedly observed runoff through seepage faces at the inlet to the upper weir in CB1 and at the channel head upslope of the CB2 weir.

Discharge through the upper weir rose within hours of natural rainfall during large storms, whereas smaller storms failed to generate increased discharge. Depending upon the size of the storm, discharge declined to preevent levels within 1 to several days in the upper weir and more slowly in the CB2 weir. A plot of maximum 24-hour precipitation versus total storm rainfall (Figure 11) illustrates that storms generating runoff through the upper weir had maximum 24-hour rainfall in excess of 20 mm and total storm rainfall in excess of 40 mm; smaller storms generated no detectable change in discharge. Although this apparent threshold for generating subsurface stormflow suggests that vadose zone storage moderates runoff, the 40 mm of rain can at most cause 80 mm of saturation given a measured 50% porosity of the colluvial soil. As the soil depth at CB1 averages 700 mm, substantial runoff occurs well before complete saturation of the soil, a result of a steep soil moisture/pressure head relation. Together these observations document consistent runoff generation by SSSF to channel heads and point to a significant influence of unsaturated response on storm runoff.

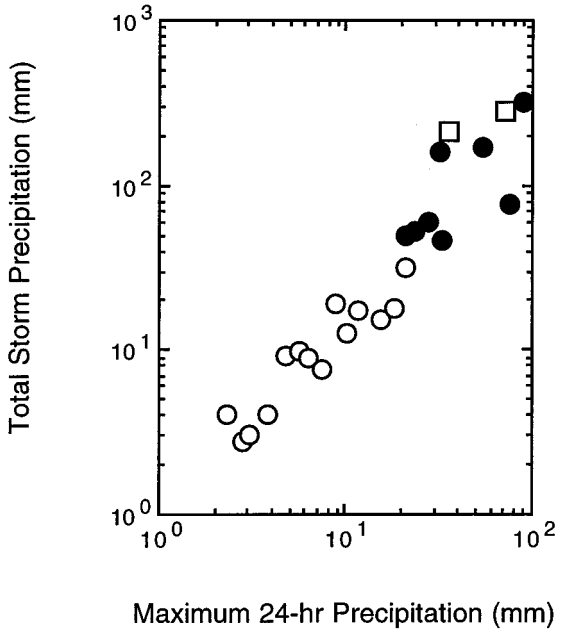

Figure 11. Plot of maximum 24-hour precipitation versus total storm precipitation for storms from January through April 1990. Open circles represent storms that did not generate runoff through the upper weir, solid circles represent storms during which a runoff peak was recorded through the upper weir, and open squares represent experiments 1 and 2.

Table 1. Runoff Coefficients

Storm Period	Upper Weir, %	Lower Weir, %	CB1 Total, %	CB2 Weir, %
Jan. 5–10, 1990	0.46			
Feb. 7–12, 1990	0.49			
March 9–14, 1990	0.38			
April 26–30, 1990	0.45			
Jan.–April 1990	0.53			0.96
1990	0.49			0.87
1991	0.29–0.34	0.33	0.62–0.67	0.88
1992	0.56	0.29	0.85	0.93
Experiment 1	0.32			
Experiment 2	0.36	0.58–0.78*	0.58–0.78	

*Includes discharge through upper weir.

Runoff Coefficients

To evaluate the amount of storm runoff generated by SSSF, we determined runoff coefficients for both natural storms and for calendar years (Table 1). Runoff coefficients were calculated for a number of storm sequences in January–April 1990, a period for which discharge and rainfall records are complete. In our analysis we defined an event as the period from initial rainfall until stage returned to the preevent level. We also calculated annual runoff coefficients for each year from 1990 to 1992. Several periods of incomplete data recovery make these calculations less accurate than the analysis of individual storms.

The two approaches used to estimate total runoff coefficients yield consistent results for the near-surface hydrologic response (Table 1). The runoff coefficient for the upper weir from January through April 1990 slightly exceeds those for individual storms. Using all available data (i.e., including periods of incomplete record), annual runoff coefficients for the upper weir were 0.49, 0.29, and 0.56 for 1990, 1991, and 1992, respectively. The low value in 1991 arises partially from the lack of much of the discharge record due to battery failure and a round from a high-caliber rifle passing through the stage recorder. Restricting the analysis to periods of overlap in the rainfall and runoff records yields a runoff coefficient of 0.34 for 1991. It appears that the upper weir recovers runoff equivalent to approximately 40–56% of the precipitation falling on CB1 during midwinter storms and over annual timescales. Runoff coefficients of 0.29–0.33 for the lower weir for the period from weir installation (October 1991) through May 1992 record the additional discharge entering the channel between the upper and lower weirs.

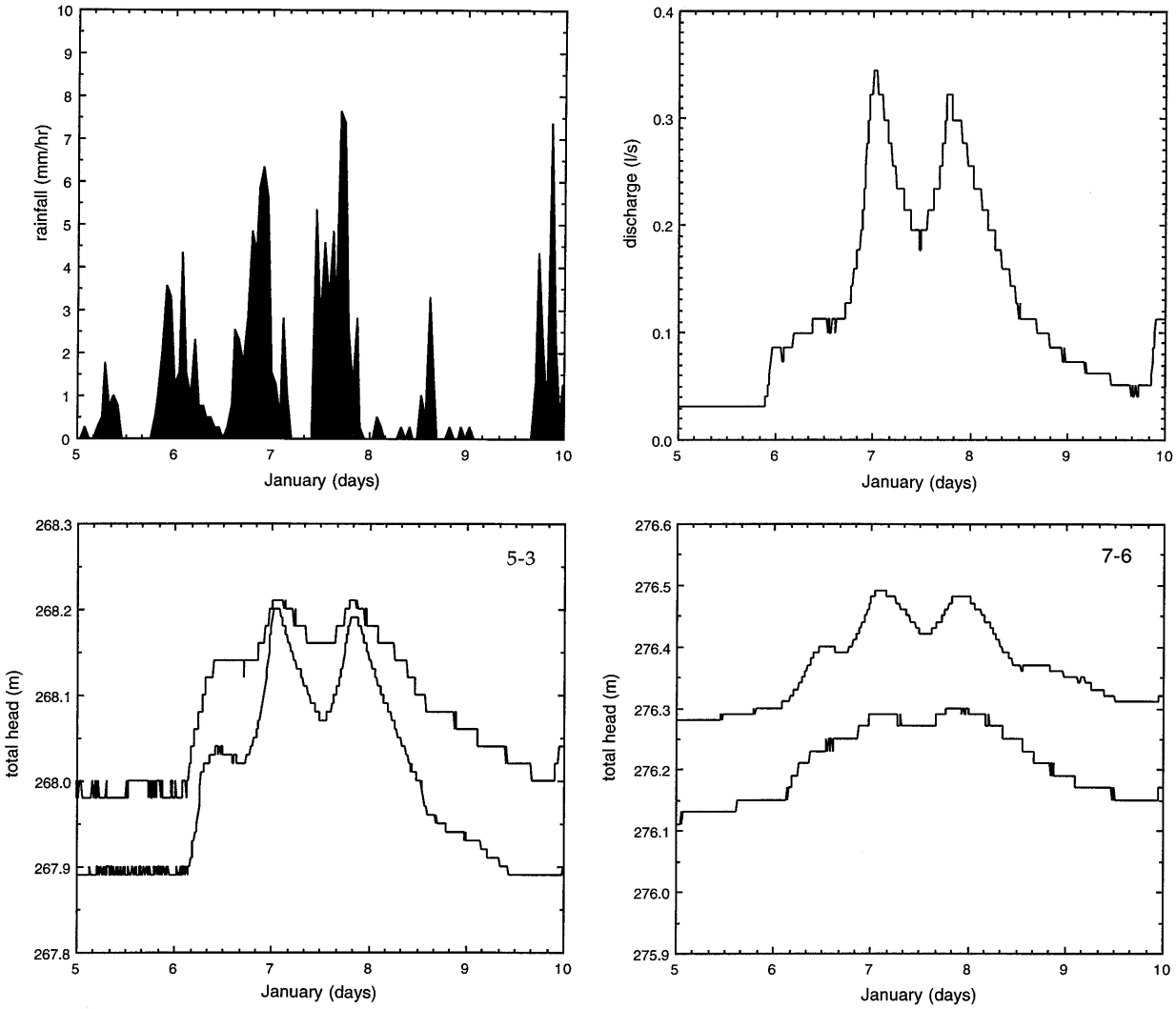

Figure 12. Hourly rainfall, discharge, and total head at nests 5-3 and 7-6 during the January 5–9, 1990, storm sequence.

The runoff record from the CB2 weir yields higher total runoff coefficients than the combined upper and lower weir discharge observed at CB1. Total runoff through the CB2 weir from January through April 1990 documents water balance during winter storms (Table 1). Limiting the analysis to periods when runoff and discharge records are complete, annual runoff coefficients for the CB2 weir are 0.87, 0.88, and 0.93 for 1990, 1991, and 1992, comparable to values of 0.77–0.92 reported for larger (2.7–12.2 km^2) forested, subsurface-flow-dominated catchments in southern British Columbia [*Cheng*, 1988]. The combined recoveries for the upper and lower weirs at CB1 and the CB2 weir constrain the combined influence of evapotranspiration and leakage to deep groundwater to less than 20% of the incident rainfall.

Piezometric Response

Intermittent manual piezometer readings during and after storms from January 1 through 9, 1990, document that most of the response occurred along the axis of the hollow where the recording piezometers are located. Hence our discussion focuses on the automated discharge and piezometric response to four storm sequences from January to April 1990. In particular, we focus on the response of nests 5-3 and 7-6, the automated nests with piezometers in both colluvium and weathered rock, to illustrate the role of variations in flow interaction on pressure head response along the hollow.

An increase in pressure head occurred in piezometer nests 5-3 and 7-6 only when 24-hour rainfall exceeded 20 mm. Once rainfall exceeds this threshold, some piezometer nests consistently exhibit recharging head gradients, while others switch from recharging to discharging during high-intensity rainfall. During the January storm sequence, maximum piezometric response at nest 5-3 occurred 2.7–4.2 hours after peak rainfall of 6.4 and 7.6 mm/h (Figure 12). In this nest, pressure head in the weathered rock rose and fell farther than in the overlying colluvium. At peak response, total head gradients almost reached hydrostatic, implying topographically driven flow and little leakage into bedrock. In contrast, the response at nest 7-6 indicates uniform recharging gradients. The deepest piezometer in nest 7-6 responded with a broad, smooth rise and fall, with less distinct peaks than in rainfall, discharge, and other piezometers. During the February storm sequence (Figure 13) the total head gradient in nest 5-3 approached hydrostatic after an initial 1-hour rainfall peak of 6.1 mm and slight discharging

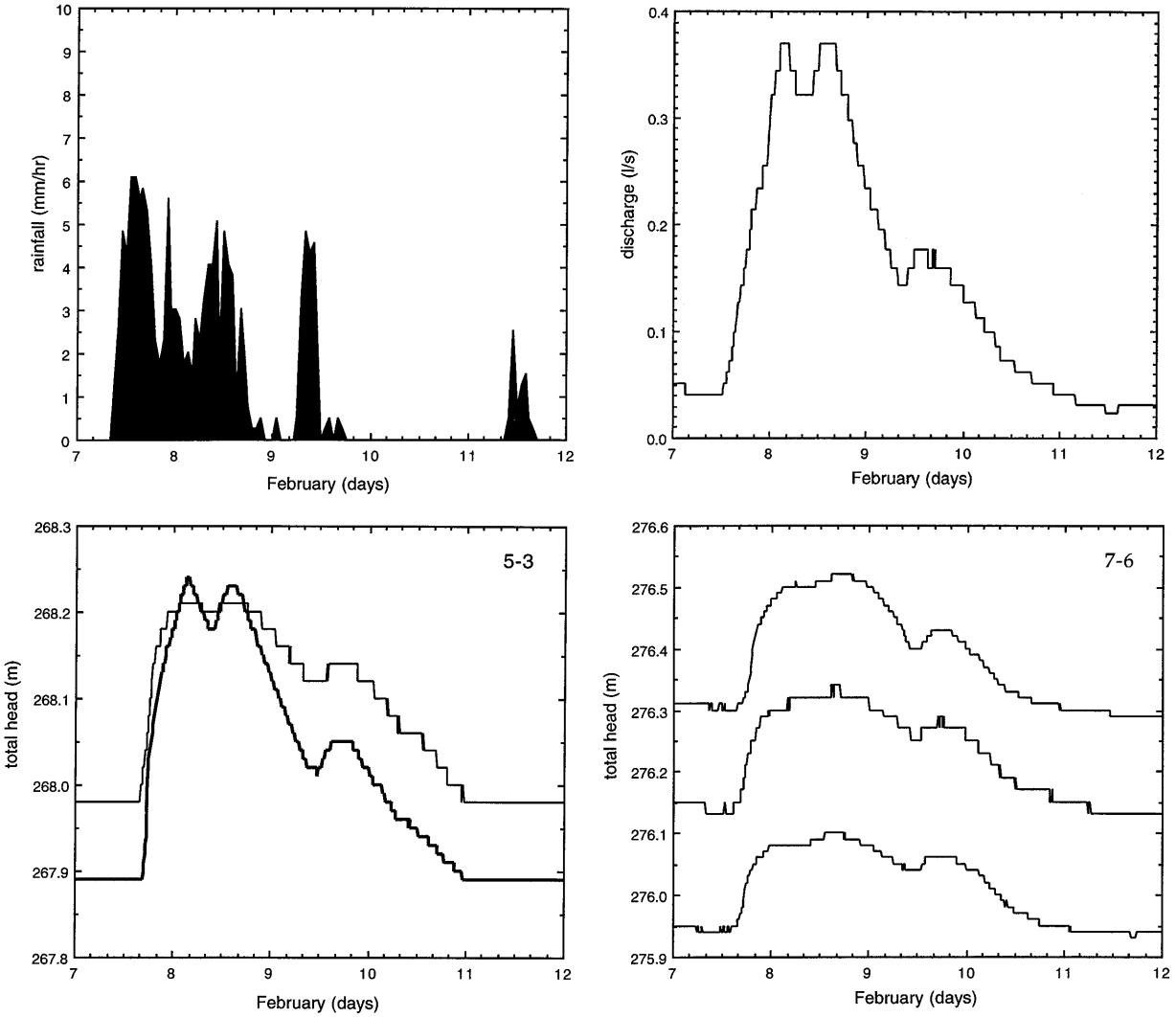

Figure 13. Hourly rainfall, discharge, and total head at nests 5-3 and 7-6 during the February 7–11, 1990, storm sequence.

gradients developed after subsequent rainfall peaks, with a lag to peak piezometric response of 5.5 ± 0.4 hours and 4.3 ± 1.2 hours. Nest 7-6 displayed recharging gradients throughout the storm sequence, and although a peak was apparent, it was less distinct than the two peaks in the discharge record. Piezometric response to the March storm occurred after rainfall with a peak 1-hour intensity of 5.6 mm/h (Figure 14). No apparent response occurred to subsequent peak 1-hour rainfall intensities of 3.8 and 2.5 mm. Again, nest 5-3 exhibited more rapid response than nest 7-6, but both nests recorded recharging gradients throughout the storm. The April storm, dominated by a single storm cell with peak 1-hour rainfall of 9.9 mm, generated the greatest discharge and piezometric response of the four storm sequences (Figure 15). Discharging gradients developed in nest 5-3 during peak piezometric response, and again nest 7-6 recorded recharging gradients throughout the storm, with a broader response in deeper piezometers. These observations from storms of different magnitude and intensity indicate that piezometric response at nest 5-3 varies from recharging during low-intensity events to discharging in response to intense rainfall, whereas nest 7-6 exhibits recharging response even during intense rainfall.

The response of nests 5-3 and 7-6 also documents two distinct styles of within storm hydrologic interaction between colluvium and the underlying bedrock. In nest 5-3, recharging gradients decrease during storm events and can reverse to discharging gradients during peak response (Figure 16). In contrast, recharging gradients increase during storm events at nest 7-6, indicating enhanced flow from the colluvium to the underlying bedrock. The maximum head gradient at nest 5-3 is strongly correlated with the maximum 6-hour rainfall intensity, and discharging gradients develop when rainfall exceeds 5 mm/h for a duration of 6 hours (Figure 17). In contrast, the head gradient at nest 7-6 is not correlated with rainfall intensity. Hence, in some locations, near-surface bedrock acts as a drain during both high- and low-intensity rainfall (nest 7-6), whereas in other locations, flow infiltrates into the underlying bedrock during low-intensity rainfall but exfiltrates from bedrock into the colluvium during high-intensity rainfall (nest 5-3).

The timing of both initial and peak piezometric response to natural rainfall varied along the hollow axis. Positive pressure head in the deepest piezometer installed in soil (i.e., immediately above the soil/bedrock contact) initiated at the channel head and progressively extended upslope. Also, peak piezo-

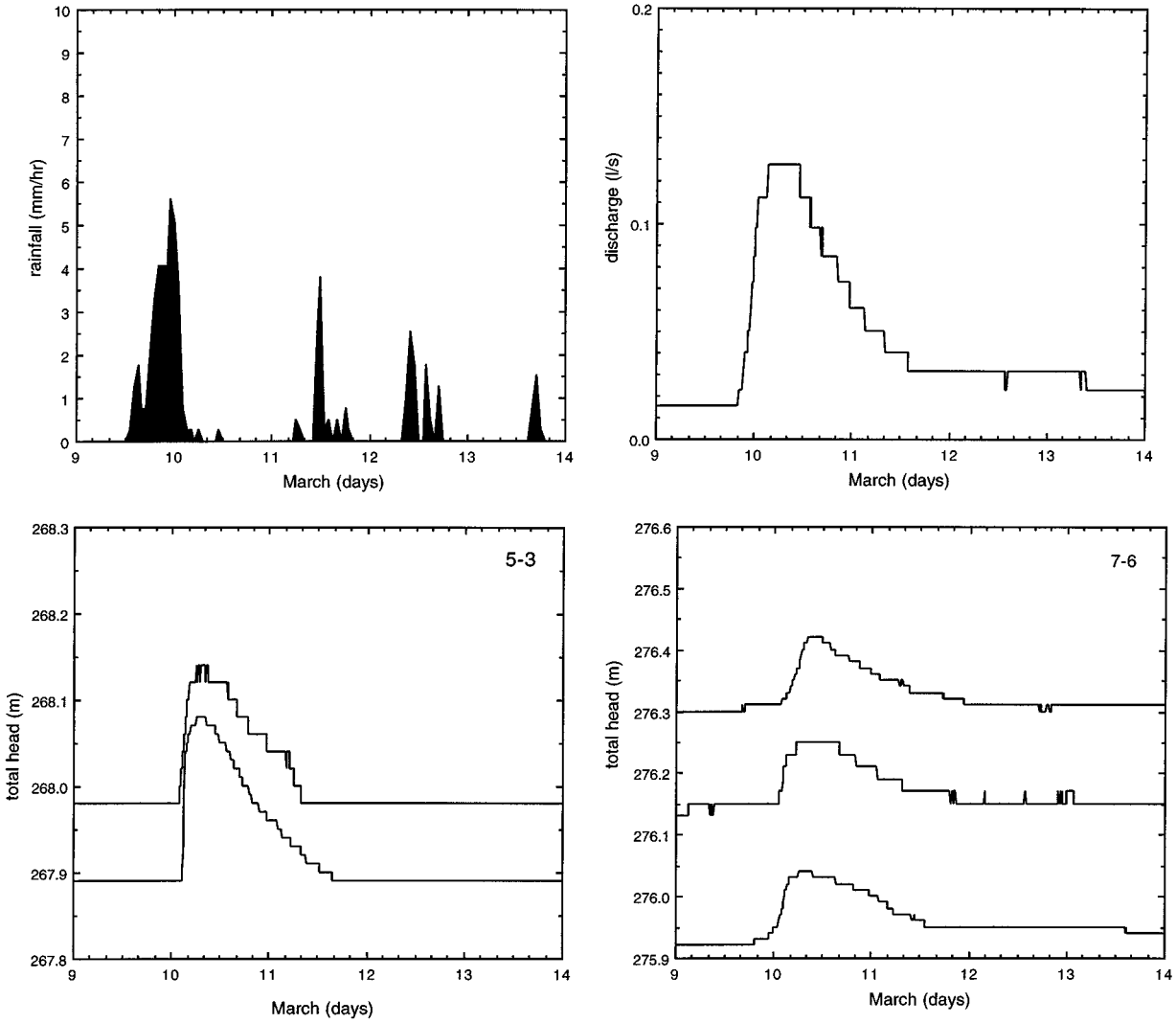

Figure 14. Hourly rainfall, discharge, and total head at nests 5-3 and 7-6 during the March 9–13, 1990, storm sequence.

metric response occurs first at the base of the slope and progressively extends upslope (Figure 18). Maximum pressure head in the area immediately upslope of the channel head occurred roughly coincident with or slightly ahead (negative values on Figure 18) of the peak discharge, but the maximum pressure head farther upslope occurred up to 12 hours after peak discharge. Shorter lag times occurred in the January and February storm sequences, events following periods of high rainfall and hence with high antecedent soil moisture. Even during those events, the peak pressure head in the 20 m upslope of the channel head occurred up to 5 hours after the peak discharge. Although the cause of this upslope delay is not certain, it could simply reflect the strong correlation between soil depth and distance upslope of the upper weir.

Discussion

Peak discharges and piezometric response at CB1 during the sprinkling experiments fell within the range observed for natural storms. Thus the more comprehensive observations from the experiments provide representative data on runoff generation. Lack of overland flow at both sites parallels other studies in steep forested terrain where highly conductive soils and moderate rainfall intensities preclude overland flow by the Hortonian mechanism [e.g., *Harr*, 1977; *Mosley*, 1979; *Tanaka et al*., 1988; *McDonnell*, 1990].

Several lines of evidence indicate that hydrologic response in the vadose zone moderates piezometric response. In particular, the rapid response of the weathered rock piezometer in nest 5-3 to the natural rainfall at the end of experiment 2 documents rapid transmittal of the rainfall signal through the vadose zone to weathered rock. The shorter time to both initial and steady state response in experiment 2 further illustrates the influence of antecedent conditions on the generation of positive pressure head. However, the 20-mm threshold rainfall necessary for generating positive pressure head represents too little rainfall to fill a significant portion of void space in the colluvium. Apparently, even relatively modest increases in soil moisture content above well-drained conditions allow pressure head spikes that arise from high-intensity rainfall pulses to rapidly propagate through the colluvium to the saturated zone.

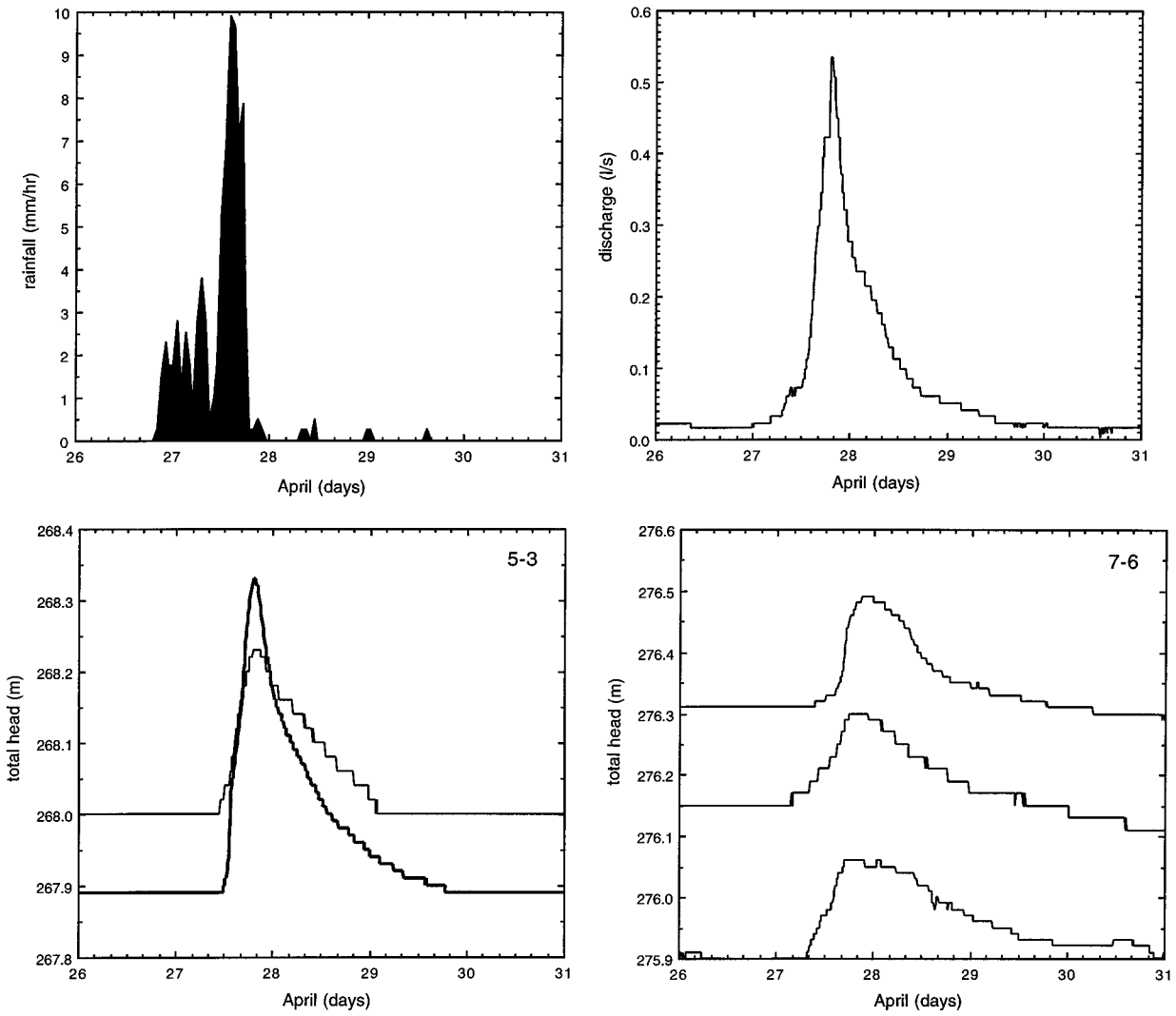

Figure 15. Hourly rainfall, discharge, and total head at nests 5-3 and 7-6 during the April 26–30, 1990, storm sequence.

R. Torres et al. (manuscript in preparation, 1996) explore more fully the mechanisms of unsaturated flow at this site.

Lack of water balance at the upper weir during winter storms and the sprinkling experiments indicates either (1) release of storage as base flow between storms, (2) evapotranspiration accounts for over half the rainfall, (3) storm flow in shallow bedrock travels under the weir, or (4) significant flow leaks to deep groundwater. If substantial rainfall is stored and released as base flow, then the seasonal and annual recovery through the weir should far exceed that for individual storms. This is not the case (Table 1). Similarly, the water balance for the CB2 weir indicates only minor leakage to deep groundwater. If evapotranspiration accounts for the partial water balance through the upper weir, then we should observe comparable water balance at and just downstream of the upper weir during the sprinkling experiments. Because we isolated the discharge through the upper and lower weirs after the sprinkling experiments, the discharge through the lower weir during natural storms includes only water that flowed beneath the upper weir and minor contributions from relatively planar side slopes downslope of the upper weir. Hence the greater discharge in the improvised lower weir than in the upper weir at the end of the second sprinkling experiment indicates substantial bedrock storm flow under the upper weir.

Additional evidence for storm flow through shallow bedrock at CB1 includes the spatially discontinuous patterns of positive pressure head in the colluvium, positive pressure head response downslope of the weir wings, and discharging gradients at nests 0-1 and 5-3. In particular, piezometric response and development of a seepage face downslope of the weir wings, which we sealed to the bedrock surface, document flow in near-surface bedrock during the sprinkling experiments. Also, the rapid and relatively in-phase response once positive pressure head develops, together with lack of evidence for depth-dependent damping of the maximum pressure head response, indicates rapid propagation of pressure signals through the saturated zone. Moreover, the in-phase response in the weathered rock and colluvium piezometers in nests 5-3 and 7-6 indicates rapid transmission of pressure signals to the weathered rock. The consistently greater response of the deepest piezometer in nest 5-3 suggests significant local contributions from the underlying bedrock over the course of individual

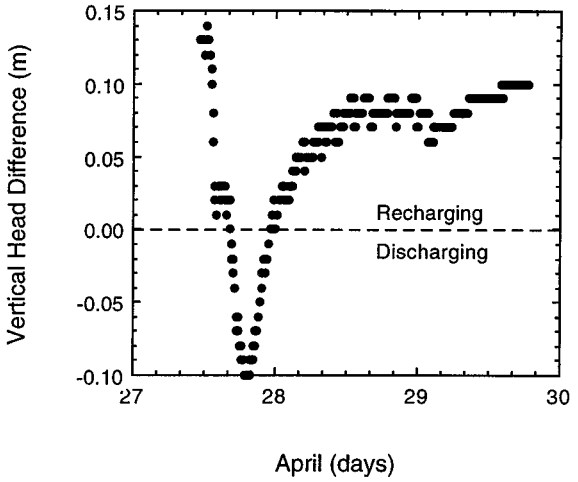

Figure 16. Difference in total head between piezometer in weathered rock and at the base of colluvium versus time for nest 5-3 during April 1990.

storm events. The observation that power drill cuttings from weir installation at the upper weir and CB2 weir were dry, even though water was running over its surface, supports the interpretation of fracture flow as the dominant bedrock runoff pathway. Oxidation staining on and around fractures in bedrock cores also indicates significant flow through some bedrock fractures. Our observations indicate significant near-surface bedrock storm flow at a site where it had been anticipated to be minimal because of apparently massive bedrock.

The pattern of saturated response within the colluvium strongly suggests interaction between flow in the bedrock and colluvium: saturated flow within the colluvium was discontinuous, partial colluvium saturation developed directly upslope from the upper weir but was of limited extent, and a distinct zone of saturated response appeared below the weir and outside the range of irrigation. The development and extent of the partial saturation just upslope of the upper weir govern the measured discharge, which only enters the upper weir from flow draining the colluvium. The depth of saturation in this patch is much greater than would be expected from direct precipitation on this area; hence water derived from upslope must exfiltrate from the bedrock. Nonetheless, the local development of this patch dictates the response of the upper weir and imparts a kind of subsurface partial area behavior to the discharge at this point. If the weir has been placed just upslope at the 265-m contour, no runoff would have been detected. If the weir had been installed at the downstream end of the first larger patch, then perhaps runoff through the upper weir would have been greater. With increasing drainage area, however, channels cut down to less conductive bedrock, thereby forcing nearly all of the runoff to surface surface, as at the CB2 weir.

Runoff chemistry at the two weirs also suggests that water emerging at the lower weir experienced more exposure to bedrock than did the water at the upper weir [*Anderson*, 1995]. Concentrations of weathering-derived solutes, such as cations, silica, and bicarbonate, as well as *p*H are consistently higher at the lower weir than at the upper weir (Figure 19). In particular, the difference in potassium concentrations between the two weirs arises from a greater influence of biotite weathering within the graywacke bedrock on the runoff at the lower weir and a greater influence of plant uptake of potassium from soil water at the upper weir. *Anderson et al.* [this issue] further explore the linkages between flow paths and runoff chemistry at CB1.

Studies of bedrock flow contributions to runoff generally focus on base flows. Studies in limestone terrain, where rapid bedrock flow might be expected, demonstrate that bedrock flow imparts significant spatial variability to base flows [*Genereux et al.*, 1993a] but also indicate that bedrock flow does not contribute significantly to storm hydrographs [*Genereux et al.*, 1993b]. Interpreted mechanisms of groundwater flow contributions to storm runoff invoke rapid mobilization of groundwater in valley bottoms and streamside areas [e.g., *Newbury et al.*, 1969; *Sklash and Farvolden*, 1979]. In upland areas, *Harr and Yee* [1975] and *Pierson* [1980] recognized the potential for significant bedrock fracture flow, and Wilson and coworkers [*Wilson and Dietrich*, 1987; *Wilson et al.*, 1990] documented the influence of variations in bedrock conductivity on pore pressures and runoff generation in a moderate-gradient hollow. Our finding of significant bedrock storm flow in an extremely steep site suggests that flow through near-surface bedrock is an important, underappreciated mechanism of runoff generation in steep, soil-mantled terrain.

We propose that spatial discontinuities in piezometric response along the hollow arise from variations in shallow bedrock fracture flow, with the gaps in positive pore pressure response due to zones of high-conductivity bedrock. Spatial variation in near-surface bedrock fractures provides an effective mechanism for generating locally elevated pressure head in highly conductive soils on steep slopes during intense rainfall, when a local downslope decrease in bedrock conductivity can drive flow upward into the overlying colluvium (Figure 20). Of the five debris flows that occurred in the vicinity of the study site during the winter of 1990, water was observed gushing out of bedrock fractures in the two scars inspected shortly after failure. Previous reports of patchy, short-lived saturated zones in colluvium on steep hillslopes emphasized rapid lateral unsaturated flow [e.g., *Harr*, 1977] and the role of variations in bedrock conductivity in draining the overlying colluvium [e.g., *Hammermeister et al.*, 1982; *Petch*, 1988]; we found no evidence of the former and our results parallel field measurements and numerical simulations [*Wilson and Dietrich*, 1987; *Wilson et al.*, 1990] that illustrate the effect of variable conductivity on flow within near-surface bedrock, pore pressure fields, and runoff generation.

The influence of near-surface bedrock conductivity on the

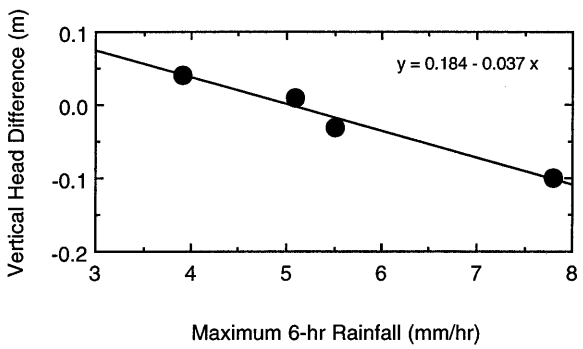

Figure 17. Vertical difference in total head at nest 5-3 versus maximum 6-hour rainfall intensity for natural storm sequences ($R^2 = 0.97$).

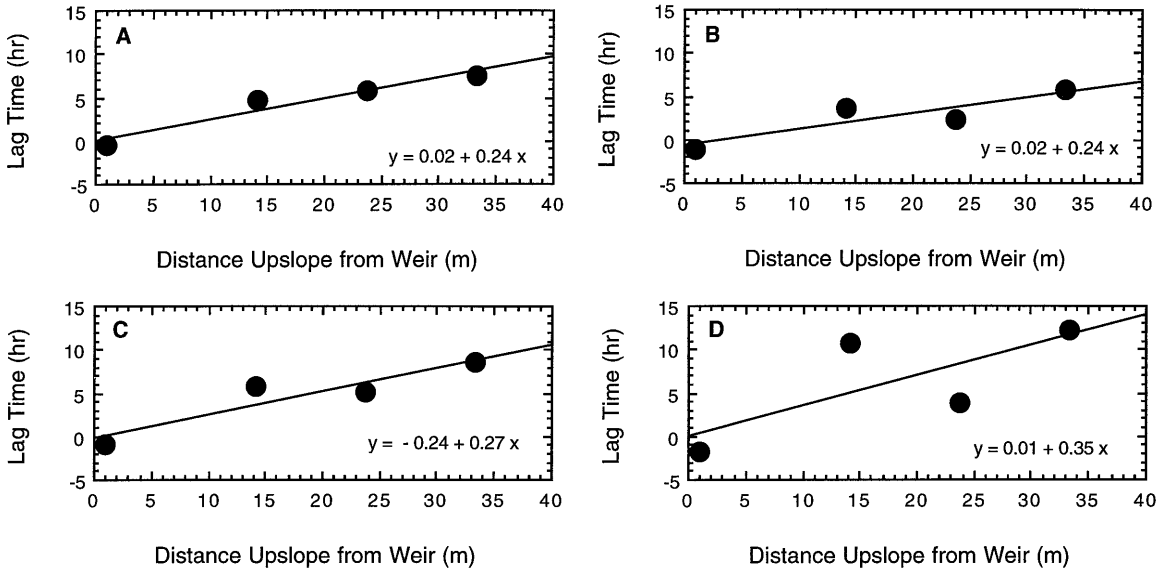

Figure 18. Lag time between peak discharge through the upper weir and peak piezometric response for automated piezometers located immediately above the soil/bedrock contact for storms in (a) January (R^2 = 0.93), (b) February (R^2 = 0.93), (c) March (R^2 = 0.86), and (d) April (R^2 = 0.54).

spatial variability of pressure head in the overlying soil has implications for landslide hazard assessment in steep terrain. Although restriction of positive pore pressures to hollows constrains zones of potential slope instability, bedrock fracture geometries may control specific sites of debris-flow initiation. At CB1 the zone of positive pressure head occurs along the hollow, indicating a dominantly topographic control on patterns of soil saturation, but the zone of piezometric response outside the weir wings was not directly downslope of the weir; flow in the fractured rock does not necessarily follow surface topography. Where there is strong coupling of flow in the near-surface bedrock and overlying colluvium, prediction of local piezometric response requires detailed knowledge of the near-surface bedrock fracture pattern. This linkage implies that slope stability models necessarily involve large uncertainties because we cannot hope to represent accurately the site-specific details of fracture flow in landscape-scale hydrological and geomorphological models. Spatially distributed hydrologic and slope stability models can predict topographic influences on shallow landsliding [e.g., *Okimura and Ichikawa*, 1985; *Okimura and Nakagawa*, 1988; *Dietrich et al*., 1992, 1993; *Montgomery and Dietrich*, 1994; *Wu and Sidle*, 1995], but variations in bedrock fracture patterns complicate prediction of where landslides occur within slide-prone areas.

Conclusions

Development of patchy saturated flow within the colluvium, saturation in the unirrigated area downslope of the weir wings, the contrast between partial water balance at the upper weir and water balance at the CB2 weir, significant flow beneath the upper weir recorded by the lower weir, and local development of discharging pressure heads during intense rainfall all indicate substantial storm runoff through near-surface bedrock. The importance of shallow bedrock flow as a component of the storm hydrograph is surprising for steep catchments with highly conductive soils overlying relatively massive bedrock. Less surprising is the result that initial piezometric response is

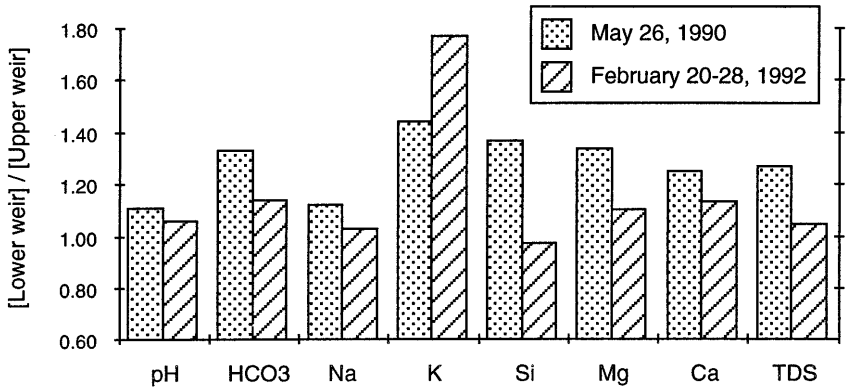

Figure 19. The ratio of *p*H and of solute concentrations at the lower weir and upper weir generally exceeds 1. Data shown are average for three pairs of samples collected on May 26, 1990, during sprinkler experiment 2 and for 10 pairs of samples collected during a natural storm in February 1992 [*Anderson*, 1995].

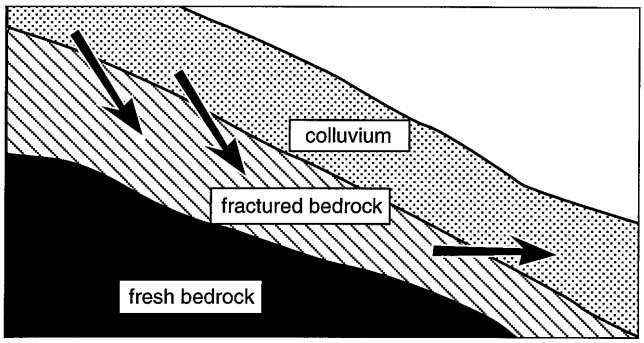

Figure 20. Schematic illustration of the interaction of flow in near-surface bedrock and overlying colluvium.

depth dependent and more rapid under wet conditions. The conclusion that flow through shallow bedrock exerts a significant control on pore pressure development in the overlying colluvium complicates the prediction of locations of shallow landsliding. The finding that upslope piezometers peak significantly after the peak discharge also holds important implications for hydrological modeling and understanding landslide hazards. Our observations demonstrate the important role that spatial variation in near-surface bedrock flow can play in piezometric response, runoff generation, and shallow landsliding in mountain environments.

Acknowledgments. This project was supported by the Weyerhaeuser Company, National Science Foundation grant NSF 89-17467, and grants TFW-SH10-FY92-010 and TFW-SH10-FY94-004 from Washington State Timber-Fish-Wildlife agreement. The efforts of many people enabled this project to develop and proceed. Kate Sullivan was instrumental in developing support for this project, Jim Clarke provided logistical support crucial to its success, and Tom Hazard kept us supplied with water during the experiments. Mark Caruso, Tamara Massong, Darryl Granger, Matt Coglon, Chris Bremer, and Juan Somoano helped survey the study areas. In total, 16 people were involved in data collection and logistical support during the two experiments. We are especially indebted to Mark Caruso, Kate Sullivan, Rohit Salve, Dave Brown, Jeff Light, Deb Loewenherz, Rita Rausch, and Jim Kirchner for working long hours under stressful conditions. Preston and Michelle Holland originally identified CB1 as a candidate site for this study. Harlan Tait Associates donated soil testing services. Lee MacDonald designed and built the bedrock drilling apparatus and helped install the bedrock borings. We thank Tim Abbe, John Buffington, Kevin Schmidt, Jonathan Stock, and anonymous reviewers for critiques of a draft manuscript and Jim Kirchner for insight in the field on the partial discharge recovery during the second experiment.

References

Anderson, M. G., and T. P. Burt, The role of topography in controlling throughflow generation, *Earth Surf. Processes*, *3*, 331–344, 1978.

Anderson, S. P., Flow paths, solute sources, weathering, and denudation rates: The chemical geomorphology of a small catchment, Ph.D. dissertation, 380 pp., Univ. of Calif., Berkeley, 1995.

Anderson, S. P., W. E. Dietrich, D. R. Montgomery, R. Torres, and K. Loague, Concentration-discharge relationships in runoff from a steep, unchanneled catchment, *Water Resour. Res.*, this issue.

Baldwin, E. M., Eocene stratigraphy of southwestern Oregon, *Bull. Oreg. Dep. Geol. Miner. Ind.*, *83*, 1974.

Benda, L., The influence of debris flows on channels and valley floors of the Oregon Coast Range, U.S.A., *Earth Surf. Processes Landforms*, *15*, 457–466, 1990.

Beven, K., and M. J. Kirkby, A physically based, variable contributing area model of basin hydrology, *Hydrol. Sci. Bull.*, *24*, 43–69, 1979.

Bonell, M., and D. A. Gilmour, The development of overland flow in a tropical rainforest catchment, *J. Hydrol.*, *39*, 365–382, 1978.

Brown, G. W., and J. T. Krygier, Clear-cut logging and sediment production in the Oregon Coast Range, *Water Resour. Res.*, *7*, 1189–1198, 1971.

Burt, T. P., and D. P. Butcher, Development of topographic indices for use in semidistributed hillslope runoff models, *Z. Geomorphol. Suppl.*, *58*, 1–19, 1986.

Cheng, J. D., Subsurface stormflows in the highly permeable forested watersheds of southwestern British Columbia, *J. Contam. Hydrol.*, *3*, 171–191, 1988.

Dietrich, W. E., and T. Dunne, Sediment budget for a small catchment in mountainous terrain, *Z. Geomorphol. Suppl.*, *29*, 191–206, 1978.

Dietrich, W. E., C. J. Wilson, and S. L. Reneau, Hollows, colluvium, and landslides in soil-mantled landscapes, in *Hillslope Processes*, pp. 361–388, edited by A. D. Abrahams, Allen and Unwin, Winchester, Mass., 1986.

Dietrich, W. E., C. J. Wilson, D. R. Montgomery, J. McKean, and R. Bauer, Channelization thresholds and land surface morphology, *Geology*, *20*, 675–679, 1992.

Dietrich, W. E., C. J. Wilson, D. R. Montgomery, and J. McKean, Analysis of erosion thresholds, channel networks and landscape morphology using a digital terrain model, *J. Geol.*, *101*, 259–278, 1993.

Dott, R. H., Jr., Eocene deltaic sedimentation at Coos Bay, Oregon, *J. Geol.*, *74*, 373–420, 1966.

Dunne, T., Field studies of hillslope flow processes, in *Hillslope Hydrology*, edited by M. J. Kirkby, pp. 227–293, Wiley-Interscience, New York, 1978.

Dunne, T., and R. D. Black, Partial area contributions to storm runoff in a small New England watershed, *Water Resour. Res.*, *6*, 1296–1311, 1970.

Dunne, T., T. R. Moore, and C. H. Taylor, Recognition and prediction of runoff-producing zones in humid regions, *Hydrol. Sci. Bull.*, *20*, 305–327, 1975.

Everett, A. G., Secondary permeability as a possible factor in the orgin of debris avalanches associated with heavy rainfall, *J. Hydrol.*, *43*, 347–354, 1979.

Fredriksen, R. L., Erosion and sedimentation following road construction and timber harvest on unstable soils in three small western Oregon watersheds, *USDA For. Serv. Res. Pap. PNW-104*, 15 pp., 1970.

Genereux, D. P., H. F. Hemond, and P. J. Mulholland, Spatial and temporal variability in streamflow generation on the West Fork of Walker Branch Watershed, *J. Hydrol.*, *142*, 137–166, 1993a.

Genereux, D. P., H. F. Hemond, and P. J. Mulholland, Use of radon-222 and calcium as tracers in a three-end-member mixing model for streamflow generation on the West Fork of Walker Branch Watershed, *J. Hydrol.*, *142*, 167–211, 1993b.

Gresswell, S., D. Heller, and D. N. Swanston, Mass movement response to forest management in the central Oregon Coast Ranges, *USDA For. Serv. Resour. Bull. PNW-84*, 26 pp., 1979.

Haagen, J. T., *Soil Survey of Coos County, Oregon*, 269 pp., Soil Conserv. Serv., U.S. Dep. of Agric., Washington, D. C., 1989.

Hammermeister, D. P., G. F. Kling, and J. A. Vomocil, Perched water tables on hillsides in Western Oregon, I, Some factors affecting their development and longevity, *Soil Sci. Soc. Am. J.*, *46*, 811–818, 1982.

Harr, R. D., Water flux in soil and subsoil on a steep forested slope, *J. Hydrol.*, *33*, 37–58, 1977.

Harr, R. D., and C. S. Yee, Soil and hydrologic factors affecting the stability of natural slopes in the Oregon Coast Range, *WRRI-33*, 204 pp., Water Resour. Res. Inst., Oreg. State Univ., Corvallis, 1975.

Hewlett, J. D., and A. R. Hibbert, Factors affecting the response of small watersheds to precipitation in humid areas, in *International Symposium on Forest Hydrology*, edited by W. E. Sopper and W. H. Lull, pp. 275–290, Pergamon, Tarrytown, N. Y., 1967.

Horton, R. E., The role of infiltration in the hydrologic cycle, *Eos Trans. AGU*, *14*, 446–460, 1933.

Hursh, C. R., Storm-water and adsorption, *Eos Trans. AGU*, *17*, 301–302, 1936.

Hvorslev, M. J., Time lag and soil permeability in groundwater observations, *Bull. 36*, 50 pp., U.S. Army Corps of Eng. Waterw. Exp. Stn., Vicksburg, Miss., 1951.

Johnson, K. A., and N. Sitar, Hydrologic conditions leading to debris-flow initiation, *Can. Geotech. J.*, *27*, 789–801, 1990.

Likens, G. E., F. H. Bormann, R. S. Pierce, J. S. Eaton, and N. M. Johnson, *Biogeochemistry of a Forested Ecosystem*, 146 pp., Springer-Verlag, New York, 1977.

Loudermilk, W. C., The role of vegetation in erosion control and water conservation, *J. For*., *32*, 529–536, 1934.
MacDonald, L. H., An inexpensive, portable system for drilling into subsurface layers, *Soil Sci. Soc. Am. J*., *52*, 1817–1819, 1988.
Mathewson, C. C., J. R. Keaton, and P. M. Santi, Role of bedrock ground water in the initiation of debris flows and sustained post-flow stream discharge, *Bull. Assoc. Eng. Geol*., *27*, 73–83, 1990.
McDonnell, J. J., A rationale for old water discharge through macropores in a steep, humid catchment, *Water Resour. Res*., *26*, 2821–2832, 1990.
Mersereau, R. C., and C. T. Dyrness, Accelerated mass wasting after logging and slash burning in western Oregon, *J. Soil Water Conserv*., *27*, 112–114, 1972.
Montgomery, D. R., Channel initiation and landscape evolution, Ph.D. dissertation, 421 pp., Univ. of California, Berkeley, 1991.
Montgomery, D. R., Road surface drainage, channel initiation, and slope stability, *Water Resour. Res*., *30*, 1925–1932, 1994.
Montgomery, D. R., and W. E. Dietrich, A physically based model for the topographic control on shallow landsliding, *Water Resour. Res*., *30*, 1153–1171, 1994.
Mosley, M. P., Streamflow generation in a forested watershed, New Zealand, *Water Resour. Res*., *15*, 795–806, 1979.
Mulholland, P. J., Hydrometric and stream chemistry evidence of three storm flowpaths in Walker Branch Watershed, *J. Hydrol*., *151*, 291–316, 1993.
Newbury, R. W., J. A. Cherry, and R. A. Cox, Groundwater-streamflow systems in Wilson Creek Experimental Watershed, Manitoba, *Can. J. Earth Sci*., *6*, 613–623, 1969.
Okimura, T., and R. Ichikawa, A prediction method for surface failures by movements of infiltrated water in a surface soil layer, *Nat. Disaster Sci*., *7*, 41–51, 1985.
Okimura, T., and M. Nakagawa, A method for predicting surface mountain slope failure with a digital landform model, *Shin Sabo*, *41*, 48–56, 1988.
Okunishi, K., and T. Iida, Evolution of hillslopes including landslides, *Trans. Jpn. Geomorphol. Union*, *2*, 291–300, 1981.
O'Loughlin, E. M., Prediction of surface saturation zones in natural catchments by topographic analysis, *Water Resour. Res*., *22*, 794–804, 1986.
Onda, Y., Contrasting hydrological characteristics, slope processes and topography underlain by Paleozoic sedimentary rocks and granite, *Trans. Jpn. Geomorphol. Union*, *15A*, 49–65, 1994.
Petch, R. A., Soil saturation patterns in steep, convergent hillslopes under forest and patsture vegetation, *Hydrol. Proc*., *2*, 93–103, 1988.
Pierson, T. C., Factors controlling debris-flow initiation on forested hillslopes in the Oregon Coast Range, Ph.D. dissertation, 161 pp., Univ. of Wash., Seattle, 1977.
Pierson, T. C., Piezometric response to rainstorms in forested hillslope drainage depressions, *J. Hydrol. N. Z*., *19*, 1–10, 1980.
Sidle, R. C., Shallow groundwater fluctuations in unstable hillslopes of coastal Alaska, *Z. Gletscherkd. Glazialgeol*., *20*, 79–95, 1984.
Sklash, M. G., and R. N. Farvolden, The role of groundwater in storm runoff, *J. Hydrol*., *43*, 45–65, 1979.
Sklash, M. G., M. K. Stewart, and A. J. Pearce, Storm runoff generation in humid headwater catchments, 2, A case study of hillslope and low-order stream response, *Water Resour. Res*., *22*, 1273–1282, 1986.
Swanston, D. N., Mechanics of debris avalanching in shallow till soils in southeast Alaska, *USDA For. Serv. Res. Pap. PNW-103*, 17 pp., 1970.
Swanston, D. N., and F. J. Swanson, Timber harvesting, mass erosion, and steepland forest geomorphology in the Pacific Northwest, in *Geomorphology and Engineering*, edited by D. R. Coates, pp. 199–221, Van Nostrand Reinhold, New York, 1976.
Tanaka, T., The role of subsurface water exfiltration in soil erosion processes, in *Recent Developments in the Explanation of Erosion and Sediment Yield*, edited by D. E. Walling, *IAHS Publ*., *137*, 73–80, 1982.
Tanaka, T., M. Yasuhara, H. Sakai, and A. Marui, The Hachioji experimental basin study—storm runoff processes and the mechanism of its generation, *J. Hydrol*., *102*, 139–164, 1988.
Terajima, T., and K. Moroto, Stream flow generation in a small watershed in granitic mountain, *Trans. Jpn. Geomorphol. Union*, *11*, 75–96, 1990.
Tsukamoto, Y., and T. Ohta, Hillslope topography and runoff processes on steep forested slopes, *J. Hydrol*., *102*, 165–178, 1988.
Tsukamoto, Y., T. Ohta, and H. Noguchi, Hydrological and geomorphological studies of debris slides on forested hillslopes in Japan, in *Recent Developments in the Explanation and Prediction of Erosion and Sediment Yield*, *IAHS Publ*., *137*, 89–98, 1982.
Whipkey, R. Z., Subsurface stormflow from forested slopes, *Bull. Int. Assoc. Sci. Hydrol*., *10*, 74–85, 1965.
Wilson, C. J., and W. E. Dietrich, The contribution of bedrock groundwater flow to strom runoff and high pore pressure development in hollows, in *Erosion and Sedimentation in the Pacific Rim*, edited by R. L. Beschta et al., *IAHS Publ*., *165*, 49–60, 1987.
Wilson, C. J., W. E. Dietrich, and T. N. Narisimhan, Predicting high pore pressures and saturation overland flow in unchannelled hillslope valleys, in *Proceedings Hydrology and Water Resources Symposium*, *1989*, pp. 392–396, Inst. of Eng., Sydney, New South Wales, Australia, 1990.
Wilson, G. V., P. M. Jardine, J. D. O'Dell, and M. Collineau, Field-scale transport from a buried line source in variably saturated soil, *J. Hydrol*., *145*, 83–109, 1993.
Wu, W., and R. C. Sidle, A distributed slope stability model for steep forested basins, *Water Resour. Res*., *31*, 2097–2110, 1995.
Yee, C. S., and R. D. Harr, Influence of soil aggregation on slope stability in the Oregon Coast Ranges, *Environ. Geol*., *1*, 367–377, 1977.

S. P. Anderson, Department of Earth Sciences, University of California, Santa Cruz, CA 95064.
W. E. Dietrich and R. Torres, Department of Geology and Geophysics, University of California, Berkeley, CA 94720.
J. T. Heffner, Environmental Research, Weyerhaeuser Company, 505 N. Pearl Street, Centralia, WA 98531.
K. Loague, Department of Geological and Environmental Sciences, Stanford University, Stanford, CA 94305.
D. R. Montgomery, Department of Geological Sciences, University of Washington, Seattle, WA 98195. (e-mail: dave@bigdirt.geology.washington.edu)

(Received April 25, 1996; revised September 18, 1996;
accepted September 28, 1996.)